

RESEARCH ARTICLE

Open Access



Structure and function of the musculoskeletal ovipositor system of an ichneumonid wasp

Benjamin Eggs^{1*†} , Annette I. Birkhold^{2†} , Oliver Röhrle²  and Oliver Betz¹ 

Abstract

Background: Modifications of the ovipositor appear to have played a prominent role in defining the host range of parasitoid hymenopterans, highlighting an important contributing factor in shaping their oviposition strategies, life histories and diversification. Despite many comparative studies on the structure of the hymenopteran terebra, little is known about functional aspects of the musculoskeletal ovipositor system. Therefore, we examined all inherent cuticular elements and muscles of the ovipositor of the ichneumonid wasp *Venturia canescens* (Gravenhorst, 1829), investigated the mechanics of the ovipositor system and determined its mode of function.

Results: We found that the movements of the ichneumonid ovipositor, which consists of the female T9 (9th abdominal tergum), two pairs of valvifers and three pairs of valvulae, are actuated by a set of six paired muscles. The posterior and the anterior 2nd valvifer-2nd valvula muscles flex and extend the terebra from its resting towards an active probing position and back. The dorsal T9-2nd valvifer muscle is modified in *V. canescens* and forms distinct bundles that, together with the antagonistically acting ventral T9-2nd valvifer muscle, change the relative position of the 2nd valvifer to the female T9. Thereby, they indirectly tilt the 1st valvifer because it is linked with both of them via intervalvifer and tergo-valvifer articulation, respectively. The 1st valvifer acts as a lever arm that transfers movements to the 1st valvula. The posterior T9-2nd valvifer muscle and the small 1st-valvifer-genital membrane muscle stabilize the system during oviposition.

Conclusions: From our examination of the elements of the musculoskeletal ovipositor system of ichneumonids, we discussed leverages and muscle forces and developed a functional model of the underlying working mechanisms adding to our understanding of a key feature that has largely determined the evolutionary success of the megadiverse Ichneumonidae with more than 24,000 hitherto described species.

Keywords: Hymenoptera, Ichneumonidae, Kinematics, Muscles, Ovipositor, Parasitoid, SEM, SR- μ CT

Background

The vast majority of hymenopterans are parasitoids of other insects. Apart from oviposition, their ovipositor serves several tasks in the parasitoid lifestyle, i.e. navigating or penetrating the substrate (if the host is concealed) or the targeted egg/puparium, assessing the host, discriminating between suitable and previously parasitized hosts, piercing the host, injecting venom, oviducting the competitors' eggs and finding a suitable place for egg laying [1]. In some species, the ovipositor is also used to form a feeding tube for host feeding or

defensive stinging [2]. Undoubtedly, modifications of the ovipositor apparatus have been one of the key factors in the evolution of the parasitoids' oviposition strategies, the life histories and the enormous diversification of this large and ecologically important insect order [2–4].

The hymenopteran ovipositor consists of the female T9 (9th abdominal tergum), two pairs of valvifers and three pairs of valvulae (cf. Figs. 1a, c, 5a) derived from the 8th and 9th abdominal segments (7th and 8th metasomal segments) (morphological terms are applied according to the Hymenoptera Anatomy Ontology (HAO) [5–7]; a table of the terms used, their definitions and synonyms is given in Table 2 in the Appendix). The basally situated valvifers accommodate the operating musculature, whereas all the valvulae are devoid of intrinsic

* Correspondence: benjamin.eggs@uni-tuebingen.de

†Benjamin Eggs and Annette I. Birkhold contributed equally to this work.

¹Evolutionary Biology of Invertebrates, Institute of Evolution and Ecology, University of Tübingen, Auf der Morgenstelle 28, 72076 Tübingen, Germany
Full list of author information is available at the end of the article



musculature [8–10]. The 1st valvifers (fusion of the 8th gonocoxites with the gonangula [10]; = gonangulum, gonangula *sensu* [1]) anterodorsally are continuous with the rami of the 1st valvulae (8th gonapophyses; = lower valves *sensu* [1]). Their posterior angles articulate dorsally with the female T9 via the tergo-valvifer articulation and ventrally with the 2nd valvifers via the intervalvifer articulation. The 2nd valvifers (9th gonocoxites) extend in the form of the 3rd valvulae (9th gonostyli; = ovipositor sheaths *sensu* [1]) and are anteroventrally articulated with the 2nd valvula (fusion of the 9th gonapophyses; = upper valve *sensu* [1]) [8, 9], which is secondarily re-separated except at the apex in some parasitoid taxa [11]. The interlocked 1st and 2nd valvulae enclose the egg canal and form the terebra (= ovipositor (shaft) *sensu* [1]), which is embraced by the 3rd valvulae when not in use. The ventral surface of the 2nd valvula is interlocked with both of the 1st valvulae by a sublateral longitudinal tongue called the rhachis, which runs within a corresponding groove called the aulax along the dorsal surface of each of the 1st valvulae. This so-called olistheter system allows the three parts of the terebra to slide longitudinally relative to each other [9, 11]. The sensillar equipment of the 1st and 2nd valvulae is highly variable among parasitoid hymenopterans [2].

Despite many descriptive studies on the comparative morphology of the hymenopteran terebra [8, 9, 11, 12], the mode of function of the musculoskeletal ovipositor system has only been described in some “symphytan” families [10, 13–15], in the aculeate *Apis mellifera* Linnaeus, 1758 (Apidae) [8] and *Cryptocheilus versicolor* (Scopoli, 1763) (Pompilidae) [16], in some species of Cynipoidea [17, 18], and in a few parasitoid species of Ceraphronoidea [19] and Chalcidoidea [20–27]. However, the underlying working mechanisms of the musculoskeletal ovipositor system of the extremely diverse and species-rich superfamily of Ichneumonoidea has remained largely unexplored so far and little is known about the actuation of the various ovipositor movements that are executed during oviposition. In this study, we investigated structural, mechanical and functional aspects of the ovipositor of *Venturia canescens* (Gravenhorst, 1829) (Hymenoptera: Ichneumonidae: Campopleginae), a cosmopolitan, synovigenic [28], non-host feeding [29], solitary, koinobiont larval endoparasitoid of several moth species (Lepidoptera) [30, 31]. The oviposition behaviour (Additional file 1) is described by Rogers [32]. These parasitoid wasps coat their eggs with virus-like particles (VLPs) to circumvent their host’s immune system [33–37] and exhibit both arrhenotokous and obligate thelytokous reproduction modes [38–41]. We aimed to (1) describe the ovipositor of *V. canescens*, including all inherent

cuticular elements and muscles, (2) examine the mechanics of this musculoskeletal system, (3) determine its mode of function and (4) discuss the process of oviposition.

Results and discussion

We combined light microscopy (LM), scanning electron microscopy (SEM), synchrotron X-ray phase-contrast microtomography (SR- μ CT) and subsequent 3D image processing with muscle and leverage analyses. Based on these microscopical and microtomographical studies, we present a thorough morphological, mechanical and functional analysis of the musculoskeletal ovipositor system (Additional file 2) that steers the various movements executed by the female ichneumonid wasp during oviposition.

Cuticular elements of the ovipositor

The paired **1st valvulae** (1vv, Figs. 1a, c, e, 2a, b, e, f, g, 4d) of *V. canescens* are terminally differentiated in five apically directed sawteeth (st; Fig. 2b) of decreasing size that are used to penetrate the substrate and the host’s skin [42, 43]. Each of the 1st valvulae has a medioventral part formed into a thickened longitudinal flap that projects inwards into the egg canal (lf1; Fig. 3a; = medio-ventral seal *sensu* [16]). These thin chitinous flaps are considered to effectively seal the crack between the 1st valvulae and prevent the loss of venom and/or oviposition fluid during oviposition [11, 44–46]. The pressure of the venom squeezes the two membranes together and thus closes the seal. A transverse flap called the valvillus (vlv; Fig. 2e) protrudes from their medial walls and projects into the central egg/venom canal (cf. [32]). Segregate valvilli are typical for taxa of Ichneumonoidea but vary in shape and number between subfamilies [11, 46]. In non-aculeate Hymenoptera, they potentially serve as a stop and release mechanism for the egg by maintaining the egg in position within the terebra and blocking the egg canal [32, 43, 46] or by pushing fluids into the ovipositor, thereby creating a hydrostatic pressure that forces the egg out of the terminal portion of the egg canal [43]. The internal microsculpture of the medial walls of the egg canal consists of distally oriented scale-like structures; leaf-like ctenidia (ct; Fig. 2f) occur from the proximal basis of the valvulae to the further distally positioned region of the valvillus, where they are replaced by spine-like subctenidial setae (scts; Fig. 2g). The ctenidia help to push the deformable egg along the egg canal by alternate movements of the 1st valvulae and prevent it from moving backwards [43, 46, 47]. They are also hypothesized to deliver forward a liquid lubricant for the moving valvulae and thus reduce

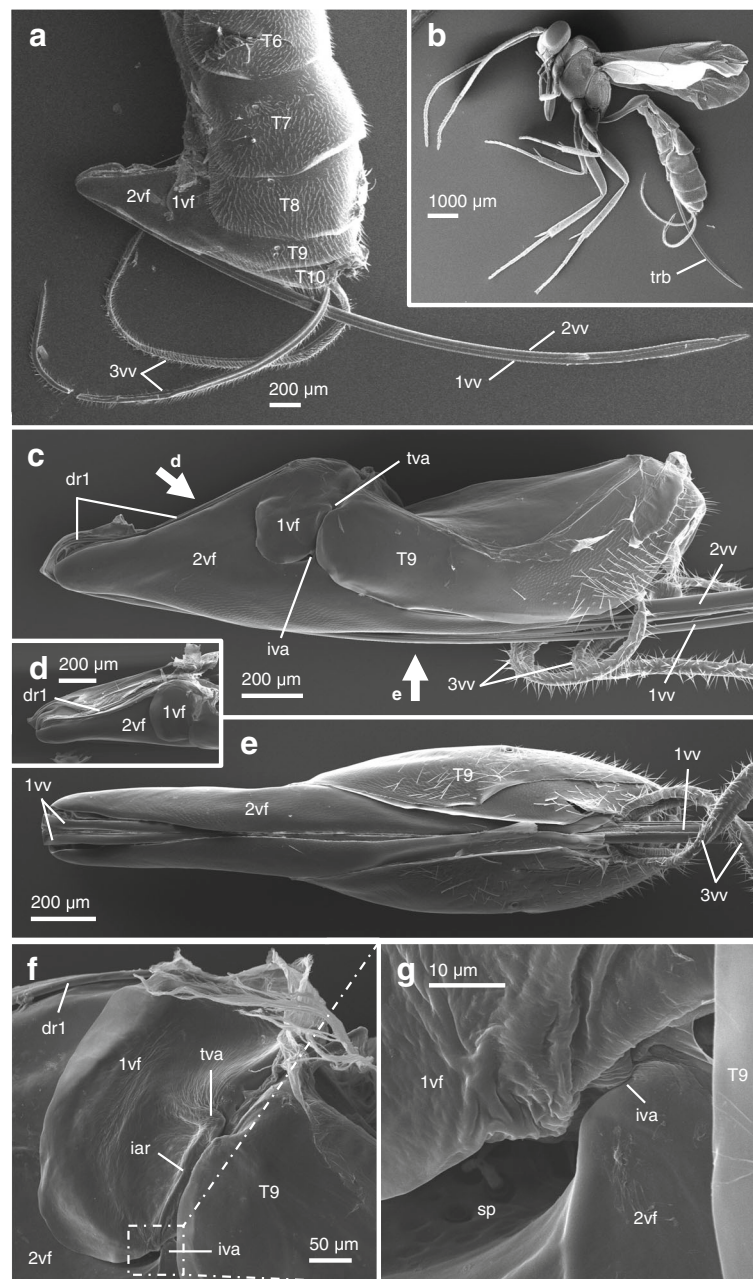


Fig. 1 SEM images of *Venturia canescens*. **a** The posterior part of the metasoma (lateral view) with the exhibited ovipositor that consists of the female T9, two pairs of valvifers and three pairs of valvulae. Because of the storage in ethanol and the drying procedure, the 3rd valvulae are coiled and do not embrace the terebra (formed by the interlocked 1st and 2nd valvulae) as in living animals (left is anterior). **b** Habitus image of *V. canescens* (lateral aspect). **c-e** Ovipositor excised from the genital chamber (left is anterior; **c**, lateral view; **d**, dorsolateral view; **e**, ventral view), so that the articulations of the 1st valvifer and the female T9 (tergo-valvifer articulation) and of the 1st valvifer with the 2nd valvifer (intervalvifer articulation) become visible. The dorsal rami of the 1st valvulae are continuous with the 1st valvifers. The fat arrows represent the direction of view of the other SEM images. **f-g** Detailed images of the tergo-valvifer and the intervalvifer articulation (lateral view, left is anterior) and the sensillar patch of the 2nd valvifer (in **g**). Abbreviations: 1vf, 1st valvifer; 1vv, 1st valvula; 2vf, 2nd valvifer; 2vv, 2nd valvula; 3vv, 3rd valvula; dr1, Dorsal ramus of the 1st valvula; iar, Interarticular ridge of the 1st valvifer; iva, Intervalvifer articulation; sp, Sensillar patch of the 2nd valvifer; T6, 6th abdominal tergum; T7, 7th abdominal tergum; T8, 8th abdominal tergum; T9, Female T9; T10, 10th abdominal tergum; tva, Tergo-valvifer articulation

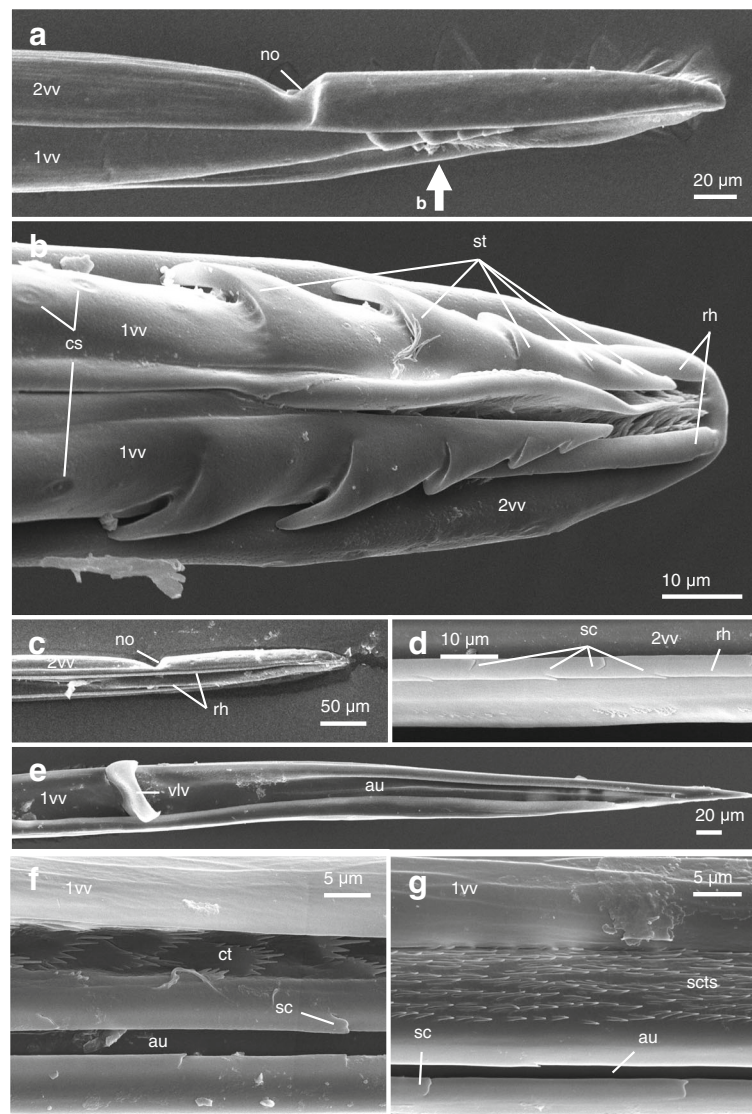


Fig. 2 SEM images of *Venturia canescens* (left is anterior). **a, b** The apex of the terebra (**a**, lateral view; **b**, ventral view; for a transverse section see Fig. 3) showing the notch and the rhachis, which ends at the very apex of the 2nd valvula, and five sawteeth directed apically and decreasing in size apically on each of the 1st valvulae. The valvulae bear various types of sensilla with the campaniform sensilla being numerous at the apices of both the 1st and the 2nd valvulae. **c** Upon removal of the 1st valvulae, the rhachises at the ventral side of the 2nd valvula become visible (ventrolateral view). **d** The rhachises show distally directed scales/serrations. **e** The inner surface of the apex of the right 1st valvula shows a single valvillus and the aulax. **f, g** The egg canal formed by the 1st and 2nd valvifers bears a microsculpture consisting of distally oriented ctenidia (**f**), which become further distally replaced by spine-like subctenidial setae (**g**) at the apex of the terebra. The aulaces of the 1st valvulae, similar to the rhachis, show distally oriented scales. The fat arrow in **a** represents the direction of view of the image in **b**. Abbreviations: 1vv, 1st valvula; 2vv, 2nd valvula; au, Aulax; cs, Campaniform sensilla; ct, Ctenidium; no, Notch; rh, Rhachis; sc, Scales; scts, Subctenidial setae; st, Sawtooth; vlv, Valvillus

friction between the valvulae during oviposition [42, 45, 46, 48].

The **2nd valvula** (2vv; Figs. 1a, c, 2a, b, c, d, 4d) is bulbous at its proximal end and basally articulated with the 2nd valvifers via the basal articulation (ba; Fig. 4i; blue region in Fig. 3). There are openings on each of the dorsolateral sides of the bulbs that presumably enable the passage of eggs, venom and other

fluids. The dorsal ramus of the 2nd valvula extends along its dorsal margin and bears the processus articularis (pra; Fig. 5h) laterally at its proximal part (anterior) and the processus musculares (prm; Fig. 5h) dorsally. On its ventral side, the 2nd valvula bears the rhachises (rh; Fig. 2b, c, d), which are interlocked with both the aulaces (au; Fig. 2e, f, g) on the dorsal side of the opposing paired 1st valvulae via the olistheter

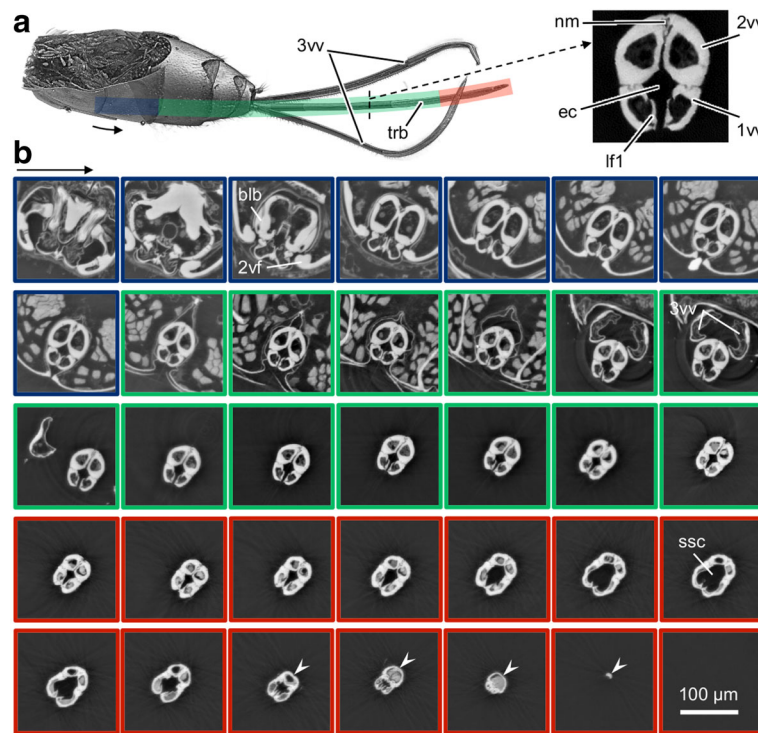
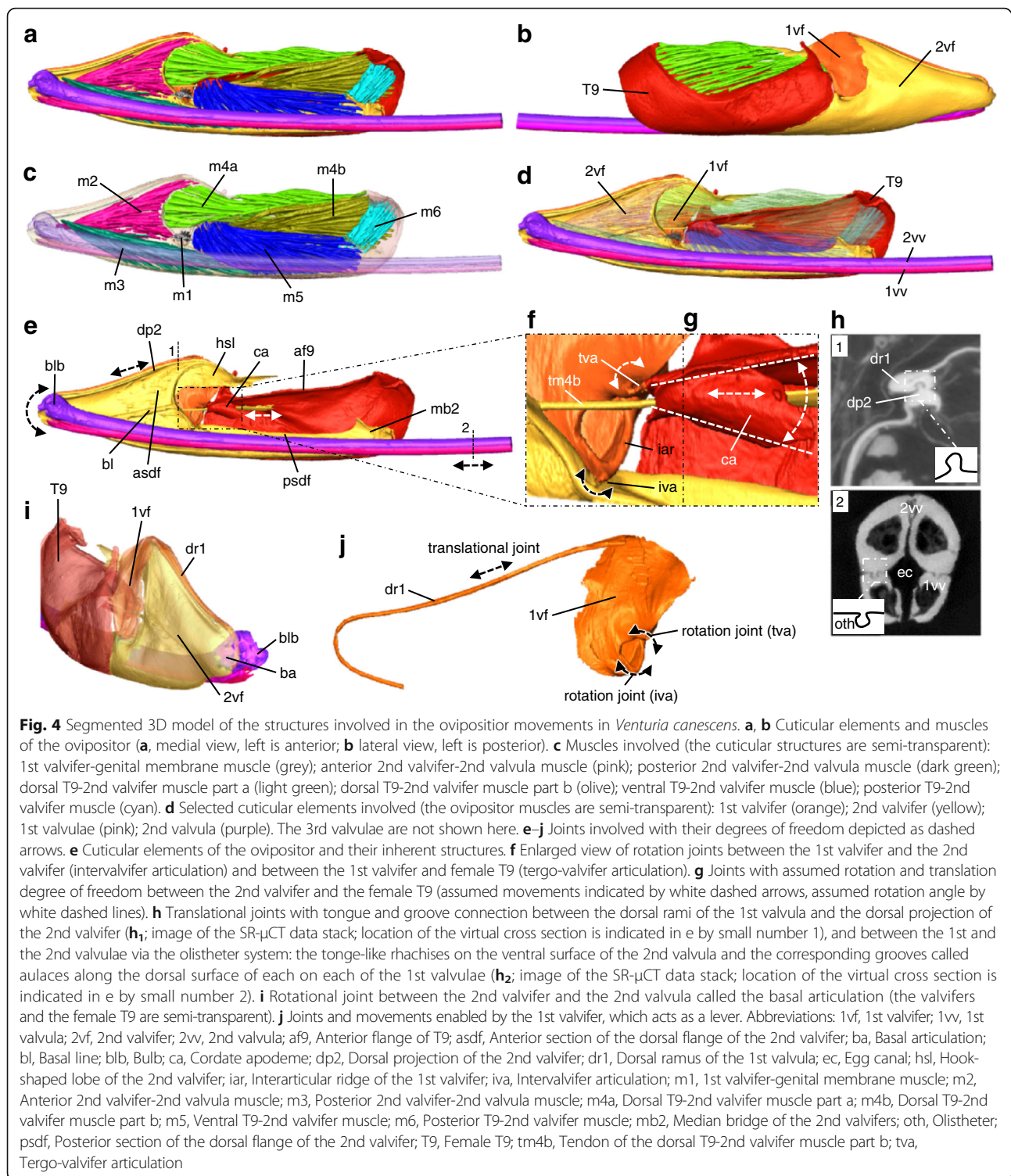


Fig. 3 SR- μ CT images of the terebra of *Venturia canescens*. **a** 3D visualization of the whole terebra in the metasoma. **b** Virtual cross sections through the terebra from proximal to distal. Proximal (blue); every 65 μ m, a cross section is displayed because of strong morphological changes such as the bulbous proximal end of the 2nd valvula. According to the limited morphological changes along the longitudinal axis, for the next part (green), a cross section is shown only every 260 μ m over the next 3380 μ m. The most distal 900 μ m (red) shows, once again, large morphological variations such as the spindle-shaped cavity formed by all three valvulae; therefore, a cross section is shown every 65 μ m. The arrows indicate the undivided distal parts of the 2nd valvula. Abbreviations: 1v1, 1st valvulae; 2v1, 2nd valvulae; 2vf, 2nd valvifer; 2vv, 2nd valvulae; 3vv, 3rd valvulae; b1b, Bulb; ec, Egg canal; lf1, Longitudinal flap of the 1st valvulae; nm, Notal membrane; ssc, Spindle-shaped cavity; trb, Terebra

system (oth; Fig. 4h₂), which extends all the way to the apex. The 2nd valvula of *V. canescens* and other ichneumonids (e.g. taxa belonging to the subfamilies of Campopleginae, Cremastinae, Ctenopelmatinae, Neorhacodinae and Tryphoninae) consists of two halves that are joined together for the most of their length by a dorsal notal membrane (nm; Fig. 3a; cf. [32, 45]) but are fused at the apex [11], so that the 2nd valvula possesses a lumen that is undivided at the apex of the terebra (arrows in red region of Fig. 3b) but that splits into two lumina for a substantial proportion of its proximal part. The blunt tip of the 2nd valvula dorsally possesses a distal notch (no; Fig. 2a, c), which is assumed to be associated with moderating penetration of the host cuticle [42] or to maintain a grip on the inner surface of the host cuticle and thereby providing a momentary clamping mechanism in the host's skin to ensure continuous engagement with the host during oviposition [43]. Almost all ichneumonid species with a pre-apical notch are larval endoparasitoids of holometabolous insects [43]. At their external surface, both the 1st and the 2nd valvulae of *V. canescens* exhibit campaniform sensilla (cs; Fig. 2b),

which are concentrated at the apices of the valvulae, especially distally of the distal notch of the 2nd valvula and posteriorly of the sawteeth of the 1st valvulae (cf. [45]). However, the sensillar equipment of the terebra was not further investigated in this study (but see [49]).

The **terebra** (trb; Fig. 1b, 3) consists of the paired 1st valvulae and the 2nd valvula, which are tightly interlocked by the olistheter (oth; Fig. 4h₂). The distally directed scales/serrations on the surfaces of both the rhachises and the walls of the aulaces (sc; Fig. 2d, f, g) potentially reduce friction forces by minimizing the contact area of the olistheter elements [46]. However, we hypothesize that these scales might also serve other functions: (1) they, analogous to the ctenidia, might forward a liquid lubricant from the metasoma to the apex of the olistheter system to reduce friction between the moving valvulae (cf. [48]), and/or (2) they might create anisotropic conditions in the olistheter by increasing frictional forces whenever a valvula is pushed in proximal direction, thereby preventing the 1st valvulae from randomly sliding back during piercing/drilling. The terebra extends far beyond the tip of



the metasoma. The diameter of the terebra decreases from the proximal to its distal end, although the part in between remains similar in diameter throughout. The cross sections of both the 1st and the 2nd valvulae are notably different across the length of the terebra

(Fig. 3b). The egg canal is largely defined by the 1st valvulae but its dorsal side is formed by the 2nd valvula (ec; Fig. 3a). At the apex of the terebra, the 1st valvulae are enlarged and form an approximately spindle-shaped cavity (ssc; red region in Fig. 3) that is

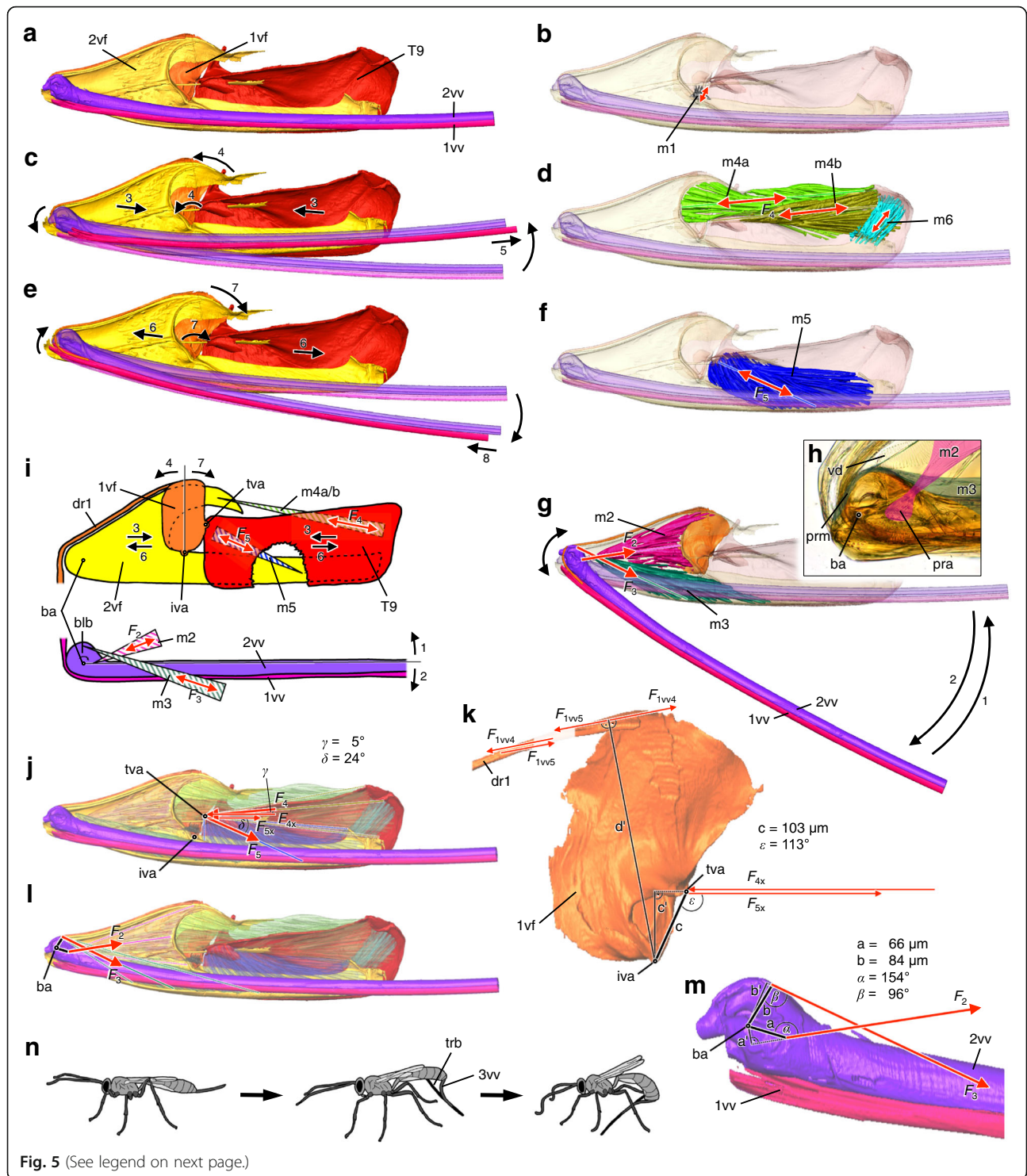


Fig. 5 (See legend on next page.)

(See figure on previous page.)

Fig. 5 Mechanics of the musculoskeletal ovipositor system of *Venturia canescens*. **a–g, i** Kinematics of the musculoskeletal ovipositor system; acting (input) muscle forces are visualized by solid red arrows (**b, d, f, g, i**) and resulting (output) movements by solid black arrows (**c, e, g, i**). **a–g, j–m** 3D model of the ovipositor system (medial view, left is anterior). **b** m1 potentially serves as a tensor muscle for stabilization of the ovipositor system during oviposition. **c, d, i** Contraction of both m4a and m4b (F_4 in **d, i**) moves the 2nd valvifer posteriorly and the female T9 anteriorly towards each other (small number 3 in **c, i**), thus indirectly causing the 1st valvifer to tilt anteriorly (small number 4 in **c, i**). This is possible because the 1st valvifer is articulated with both the 2nd valvifer and the female T9 via the intervalvifer and tergo-valvifer articulations that act as rotational joints. The 1st valvifer thereby functions as a lever arm that transfers the movement to the dorsal ramus of the 1st valvula and consequently causes the 1st valvula to slide distally relative to the 2nd valvula (small number 5 in **c**). These movements might also facilitate the extension of the terebra back towards its resting position (**c**). m6 thereby stabilizes the ovipositor system by holding the 2nd valvifer and the female T9 in position and preventing them to rotate around the articulations (**d**). **e, f, i** Contraction of m5 (F_5 in **f, i**) moves the 2nd valvifer anteriorly and the female T9 posteriorly apart from each other (small number 6 in **e, i**), thus causing the 1st valvifer to tilt posteriorly (small number 7 in **e, i**) and consequently causing the 1st valvula to slide proximally relative to the 2nd valvula (small number 8 in **e**). These movements might also facilitate the flexion of the terebra (**e**). **g, i** Contraction of m3 (F_3 in **g, i**) causes the bulbs to pivot anteriorly at the basal articulation, thus flexing the 2nd valvula and, therefore, the whole terebra (small number 2 in **g, i**). Contraction of m2 (F_2 in **g, i**) extends the terebra back towards its resting position (small number 1 in **g, i**). **h** Light microscopical image of the insertion regions of m2 and m3 at the processus articularis and the processus musculares, respectively (lateral view, left is anterior). The duct of the venom gland reservoir of the 2nd valvifer ends at the lateral openings of the bulbous region of the 2nd valvula. **i** Resulting schematic drawing of the mechanism of the tilting movements of the 1st valvifer and of the flexion/extension of the terebra (lateral view, left is anterior, not to scale). Only the two pairs of antagonistically acting muscles that are mainly responsible for these movements are represented in simplified terms (m2/m3 and m4/m5). The muscles stabilizing the system (m1 and m6) are not depicted here. **j–m** Simplified mechanical scheme of the leverages of the ovipositor in the resting position; acting (input) muscle forces are visualized by solid red arrows, their horizontal force vector components and the resulting (output) forces by thin red arrows (**j, k**), the anatomical (in)levers by solid black lines and the effective (= mechanical) levers by thin black lines, and the joint angles ($\alpha, \beta, \varepsilon$) are given (**k, m**). **j, l** Major direction of the acting muscle forces (F_2, F_3, F_4 and F_5) from a muscle's insertion point to the centre point of its origin. **j, k** Under the simplified assumption that the 2nd valvifer, which acts as the frame of reference, and the female T9 are guided and cannot twist but only move towards or apart from each other along the horizontal anterior–posterior axis, the input force vectors F_{4x} and F_{5x} act horizontally at the 1st valvifer at the tergo-valvifer-articulation. The distance between the tergo-valvifer articulation (where the force is applied) and the intervalvifer articulation (joint axis/pivot point) is the anatomical inlever c ; for torques see eqs. 4, 5. The 1st valvifer acts as a lever with the effective outlever d' , resulting in pro- or retraction forces at the dorsal ramus of the 1st valvula F_{1vw} and F_{1ws} ; see eqs. 6, 7. **l, m** Input force vectors F_2 and F_3 acting at the proximal end of the 2nd valvula with the basal articulation as joint axis and the anatomical inlevers a and b ; for torques see eqs. 2, 3. **n** Schema of a female wasp flexing its terebra to an active position for oviposition (after [32]) (Additional file 1), which might be supported by the flexible 3rd valvulae (not shown in a–m). Abbreviations: 1vf, 1st valvifer; 1vv, 1st valvula; 2vf, 2nd valvifer; 2vv, 2nd valvula; 3vv, 3rd valvula; ba, Basal articulation; blb, Bulb; dr1, Dorsal ramus of the 1st valvifer; F , Force; F_x , Horizontal vector components of a force; iva, Intervalvifer articulation; m1, 1st valvifer-genital membrane muscle; m2, Anterior 2nd valvifer-2nd valvula muscle; m3, Posterior 2nd valvifer-2nd valvula muscle; m4a, Dorsal T9-2nd valvifer muscle part a; m4b, Dorsal T9-2nd valvifer muscle part b; m5, Ventral T9-2nd valvifer muscle; m6, Posterior T9-2nd valvifer muscle; pra, Processus articularis; prm, Processus musculares; T9, Female T9; trb, Terebra; tva, Tergo-valvifer articulation; vd, Duct of the venom gland reservoir of the 2nd valvifer

partly occluded by the valvilli of each of the 1st valvulae (cf. [32]).

The paired **3rd valvulae** (3vv; Figs. 1a, c, e, 3) emerge at the posterior end of the 2nd valvifer and ensheath and protect the terebra when at rest. The lateral walls of the 3rd valvulae of *V. canescens* and other parasitoid wasps with long external terebrae are annulated by fine transversal narrow furrows (cf. [50]), which makes them flexible and allow their extensive deformation during oviposition. Since the valvulae lack intrinsic muscles, deformation must arise as a passive response to external pressures. The ability to bend the 3rd valvulae facilitates oviposition [50], however, it is not yet clear if *V. canescens* is able to support the flexion of the terebra towards an active probing position and its steering during the search for a potential host with their 3rd valvulae or if they simply follow the movements of the terebra (Fig. 5n; Additional file 1; cf. [32]). The distally directed dense microsetae on the inner surface of the 3rd valvulae (cf. [45]) are thought to be involved in cleaning the ovipositor sensilla between oviposition

episodes [2, 12, 50]. The 3rd valvulae potentially also have a sensory function [1].

The paired **1st valvifers** (1vf; Figs. 1a, c, d, f, g, 4b, d, j) of *V. canescens* and other ichneumonid species are short and show an almost oblong shape (with rounded edges) [8], unlike the bow-shaped 1st valvifers of species of Chalcidoidea [21, 23–26] or the triangularly shaped 1st valvifers of species of Apoidea [8, 9, 51, 52]. The posterior angles of the 1st valvifer are doubly movably articulated with the modified female T9 via the tergo-valvifer articulation and via its posteroventral corner with the 2nd valvifer by means of the intervalvifer articulation (tva/iva; Figs. 1c, f, g, 4f, j). A strengthened ridge called the interarticular ridge (iar; Figs. 1f, 4f) occurs between the two articulations and might mechanically stabilize the 1st valvifer during oviposition. The anterodorsal angle of the 1st valvifer is continuous with the dorsal ramus of the 1st valvula (dr1; Figs. 1c, d, f, 4h₁, i, j), which is interlocked with the dorsal projection of the 2nd valvifer (dp2; Fig. 4e, h₁) by a system analogous to the olistheter. This tight

interlocking guides the dorsal rami and prevents them from buckling when pushing forces are applied during the protraction of the 1st valvulae. The rami make acute angles around the proximal bulbous end of the 2nd valvula. The cuticle in the part of the dorsal rami that slides around the angle during pro- or retraction of the 1st valvulae needs to be flexible in the sagittal plane and might contain high proportions of the very elastic rubber-like protein resilin (cf. [53–55]).

The paired **2nd valvifers** (2vf; Fig. 1a, c, e, f, g, 4b, d) are elongated and their posterior parts are placed medially of the female T9. A conjunctiva, called the genital membrane (not shown), connects the ventral margins of both the 2nd valvifers arching above the 2nd valvula. The 2nd valvifer bears the dorsal flange, which extends upon its dorsal margin and which is divided by a sharply defined ridge called the basal line (bl; Fig. 4e) into an anterior and a posterior section. The anterior section of the dorsal flange of the 2nd valvifer (asdf; Fig. 4e) dorsally bears the dorsal projection of the 2nd valvifer (dp2; Fig. 4e, h₁) and extends upwards in a hook-shaped lobe (hsl; Fig. 4e; *sensu* [8]) at its postero-dorsal end, which might allow a greater arc of movement of the 1st valvifer and therefore a greater protraction of the 1st valvulae. The dorsal margins and the dorsal flanges are strengthened by cuticular ridges that might have a stabilizing function to prevent deformation. Sensillar patches (sp; Fig. 1g) can be seen on the 2nd valvifer near the intervalvifer and the basal articulation (cf. [56]), monitoring the movements of the 1st valvifer and therefore the connected 1st valvula or the position of the bulbs of the 2nd valvula. The posterior section of the dorsal flange of the 2nd valvifer (psdf; Fig. 4e) is elongated and oriented almost vertically. At their posterodorsal ends, the 2nd valvifers are connected by the median bridge (mb2; Fig. 4e). The duct of the venom gland reservoir (vd; Fig. 5h) is situated in between the paired 2nd valvifers.

The **female T9** (T9; Figs. 1a, c, e, f, g, 4b, d) is elongated and anterodorsally bears a hook-shaped structure. Medially at its anterior end, the T9 forms a funnel-like structure at the cordate apodeme (ca; Fig. 4e, f, g), situated posteriorly to the tergo-valvifer articulation. This structure has not yet been described in parasitoid hymenopterans. The anterodorsal and dorsal margins of the female T9 is strengthened by the anterior flange of T9 (af9; Fig. 4e) that might mechanically stabilize the female T9 during oviposition.

Joints of the musculoskeletal ovipositor system

The musculoskeletal ovipositor system possesses three main joints.

The **basal articulation** (ba; Fig. 4i) connects the laterally placed bulbs of the 2nd valvula with the thickened anteroventral parts of the 2nd valvifers via a rotational joint. This joint might also allow some limited pivoting movements of the 2nd valvula and therefore of the whole terebra.

Both the 2nd valvifer and the female T9 are connected with the 1st valvifer by the **intervalvifer articulation** and the **tergo-valvifer articulation** (iva/tva; Figs. 1c, f, g, 4f, j), respectively, forming a double joint. The tergo-valvifer articulation is situated dorsal to the intervalvifer articulation. Both of these articulations act as rotational joints; thus, the 1st valvifer is movable in the sagittal plane only.

Ovipositor muscles

The maximum tensions at constant muscle length (isometric tension) that individual insect muscles can exert greatly vary between species, ranging from 19 to 700 kPa [57, 58] (e.g. approximately 38 kPa exerted by the asynchronous dorso-ventral flight muscle in *Bombus terrestris* (Linnaeus, 1758) at 30 °C [59]). In case of parallel muscle fibres, the maximum force (F) created by a muscle can be estimated by using the specific tension (f) and the mean cross section area (CSA; Table 1) according to the equation:

$$F = \text{CSA} \cdot f \quad (\text{eq. 1})$$

However, there are, to the best of our knowledge, no studies hitherto that measured tensions of abdominal muscles of hymenopterans we could refer to.

The ovipositor of *V. canescens* possesses a set of six paired muscles (Fig. 4c; Table 1), one of them (m4) forming two distinct bundles.

The paired **1st valvifer-genital membrane muscles** (m1) are the only muscles of the 1st valvifer. They originate at the medial surface of the posteroventral part of the 1st valvifer, i.e. between the tergo-valvifer and the intervalvifer articulation, and insert anteriorly on the genital membrane. They are the smallest muscles of the ovipositor with a CSA of 0.0008 mm² each (Table 1).

The paired fan-shaped **anterior 2nd valvifer-2nd valvula muscles** (m2) arise at the medial region along the anterodorsal part of the 2nd valvifer, largely at the anterior section of the dorsal flange (asdf; Fig. 4e), and insert at the processus articularis (pra; Fig. 5h), a process that extends laterally from the proximal part of the 2nd valvula to form the medial part of the basal articulation. These muscles have a CSA of 0.0032 mm² each (Table 1).

The paired **posterior 2nd valvifer-2nd valvula muscles** (m3) originate at the medial region along the ventral part of the 2nd valvifer and insert at the

Table 1 Ovipositor muscles of *Venturia canescens*. The muscles (abbreviations in brackets), their origin, insertion and assumed function are described. In addition, the measured volume, mean length and the mean cross section area (CSA) of the single muscles are listed

muscle name (label)	origin	insertion	assumed function	volume [mm ³]	mean length [mm]	mean cross section area (CSA) [mm ²]
1st valvifer-genital membrane muscle (m1)	medial surface of the posteroventral part of the 1st valvifer, in the centre between the tergo-valvifer and the intervalvifer articulation	anteriorly on the genital membrane	tensor muscle for stabilization of the 1st valvifers during ovipositor movements	0.0001	0.175	0.0008
anterior 2nd valvifer-2nd valvula muscle (m2)	medial region along the anterodorsal part of the 2nd valvifer	at the processus articularis	extensor of the terebra (towards the resting position)	0.0015	0.455	0.0032
posterior 2nd valvifer-2nd valvula muscle (m3)	medial region along the ventral part of the 2nd valvifer	at the processus musculares	flexor of the terebra (towards the active probing position): causes the bulb to pivot anteriorly at the basal articulation	0.0029	0.760	0.0039
dorsal T9-2nd valvifer muscle part a (m4a)	lateral region along the posterodorsal part of the anterior margin of female T9	anterior section of the dorsal flange of the 2nd valvifer, partly at the dorsal hook-shaped lobe	protractor of the 1st valvulae: moves the 2nd valvifer posteriorly and the female T9 anteriorly towards each other, causing the 1st valvifer to tilt anteriorly and thus the 1st valvula to slide distally relative to the 2nd valvula	0.0047	0.950	0.0050
dorsal T9-2nd valvifer muscle part b (m4b)	medial region along the posterodorsal part of the anterior margin of female T9	anterior section of the dorsal flange of the 2nd valvifer via tendon, ventrally to m4a	retractor of the 1st valvulae: moves the 2nd valvifer anteriorly and the female T9 posteriorly apart from each other, causing the 1st valvifer to tilt posteriorly and thus the 1st valvula to slide proximally relative to the 2nd valvula	0.0029	0.740	0.0039
ventral T9-2nd valvifer muscle (m5)	medial region of the anterodorsal part of female T9, partly on the cordate apodeme	along the posterior section of the dorsal flange of the 2nd valvifer	muscle for stabilization by holding the posterior parts of the 2nd valvifers in position during ovipositor movements	0.0062	0.805	0.0077
posterior T9-2nd valvifer muscle (m6)	medially from the posterodorsal part of female T9	median bridge of the 2nd valvifers		0.0004	0.280	0.0015

All measurements were determined directly from the 3D muscle masks of the SR- μ CT dataset. These values potentially are lower than in living animals due to shrinking artefacts. The total muscle length was determined as the distance between the centre points of the muscle attachments. CSA was determined as muscle volume / muscle length

processus musculares (prm; Fig. 5h), namely the apodeme that extends dorsally from the proximal part of the 2nd valvula to the genital membrane. These muscles have a CSA of 0.0039 mm², which is similar to that of m2 (Table 1).

The paired **dorsal T9-2nd valvifer muscles** (m4a/b) are modified in their insertion and form two distinct muscle bundles, as it is also known to occur in the ichneumonid genus *Megarhyssa* Ashmead, 1858 [8, 60]. One part of these muscles (m4a) arises at the lateral region along the posterodorsal part of the anterior margin of female T9 and inserts at the anterior section of the dorsal flange of the 2nd valvifer (asdf; Fig. 4e) and partly on the hook-shaped lobe of the 2nd valvifer (hsl; Fig. 4e). The other part (m4b) is fan-shaped and originates at the medial region along the posterodorsal part of the anterior margin of female T9. The muscle tendons (tm4b; Fig. 4f, g) also insert at the anterior section of the dorsal flange of the 2nd valvifer, ventrally to the insertion region of m4a. The tendon of m4b thereby traverses the funnel-like structure at the cordate apodeme (ca; Fig. 4f, g) of the female T9. Muscles m4a and m4b are long thick muscles with a CSA of 0.0050 mm² and 0.0039 mm², respectively (Table 1).

The paired **ventral T9-2nd valvifer muscles** (m5) arise from the medial region of the anterodorsal part of the female T9, partly at the funnel-like structure at the cordate apodeme (ca; Fig. 4f, g), and insert along the posterior section of the dorsal flange of the 2nd valvifer (psdf; Fig. 4e). These are the largest ovipositor muscles with a CSA of 0.0077 mm².

The paired **posterior T9-2nd valvifer muscles** (m6) arise medially at the posterodorsal part of the female T9 and insert at the median bridge of the 2nd valvifers (mb2; Fig. 4e). They are the second smallest muscles of the ovipositor with a CSA of 0.0015 mm² (Table 1).

The literature concerning the musculoskeletal ovipositor system of ichneumonid wasps is limited and some inconsistent statements have been made about certain ovipositor muscles. We describe the 1st valvifer-genital membrane muscle for the first time in an ichneumonid species. Either this small muscle is not present in all ichneumonid species or, more likely, previous authors (e.g. [8, 60]) might have overlooked its presence. In *Megarhyssa macrurus lunator* (Fabricius, 1781) (Hymenoptera: Ichneumonidae), Abbott [60] described the 1st valvifer-2nd valvifer muscle as 'a small muscle connecting the "runner" plate [= 2nd valvifer] with the dorsal margin of the "kidney" plate [= 1st valvifer]'. However, this muscle has neither been found in *Megarhyssa atrata* (Fabricius, 1781) (Hymenoptera: Ichneumonidae) by Snodgrass

[8] nor in *V. canescens* in the present study and might have been mistaken for the anterior 2nd valvifer-2nd valvula (m2) muscle by this author.

In general, the musculoskeletal ovipositor system of ichneumonid wasps is similar to that of the parasitoid hymenopteran species belonging to Ceraphronoidea [19], a superfamily that is closely related to Ichneumonoidea [61]. However, the ceraphronoids lack the anterior 2nd valvifer-2nd valvula muscle [19] that is present in *V. canescens* and other ichneumonids. All chalcidoid species investigated to date with regard to the ovipositor muscles (Agaonidae [26], Aphelinidae [27], Chalcididae [20], Eurytomidae [23], Pteromalidae [21, 25] and Torymidae [24]) comprise the same set of muscles as ichneumonids but lack the 1st valvifer-genital membrane muscle. All the taxa of Chalcidoidea, Ceraphronoidea and Ichneumonoidea investigated hitherto (including our study of *V. canescens*) lack the 1st valvifer-2nd valvifer muscle, lateral T9-2nd valvifer muscle, 2nd valvifer-genital membrane muscle and T9-genital membrane muscle, which have been described in other hymenopteran taxa [7].

Mechanics and mode of function of the musculoskeletal ovipositor system

The set of six paired ovipositor muscles in *V. canescens* (Fig. 4c; Table 1) comprises two pairs of two antagonistically working muscles that are mainly responsible for the various ovipositor movements, and two muscles stabilizing the musculoskeletal system. Based on the following functional model, we assume that the anterior (m2) and the antagonistically acting posterior 2nd valvifer-2nd valvula muscles (m3) extend or flex the terebra, whereas the two parts of the dorsal T9-2nd valvifer (m4a/b) and the antagonistically acting ventral T9-2nd valvifer muscle (m5) indirectly protract or retract the 1st valvulae. The relatively small 1st valvifer-genital membrane muscle (m1) and the posterior T9-2nd valvifer muscle (m6) might predominantly serve for the stabilization of the ovipositor system during oviposition.

Flexion and extension of the terebra

The 2nd valvula of *V. canescens* is connected with the 2nd valvifers by a rotational joint called the basal articulation (ba; Figs. 4i, 5h, i, l, m). Two antagonistic muscles (m2, m3) insert at the bulbous region around this articulation (Fig. 5h). The insertion region of the posterior 2nd valvifer-2nd valvula muscle (m3) at the 2nd valvula is located dorsally of the basal articulation, whereas its region of origin at the 2nd valvifer is located posteroventrally to it. Therefore, a contraction of m3 (F_3 ; Fig. 5g, i) causes the

bulbs (blb; Fig. 4e, i) to pivot anteriorly at the basal articulation. This leads to a flexion of the 2nd valvula and the interlocked 1st valvulae from its resting position between the paired 3rd valvulae towards an active probing position (small number 2; Fig. 5g, i; Table 1). An alternate contraction of m3 on either side might also cause the terebra to rotate to a certain degree. The insertion region of the anterior 2nd valvifer-2nd valvula muscle (m2) at the 2nd valvula is situated posteroventrally of both the basal articulation and the insertion region of m3, whereas its origin at the 2nd valvifer is located posterodorsally of the articulation. Hence, when m2 (F_2 ; Fig. 5g, i) contracts, the terebra is extended towards its resting position (small number 1; Fig. 5g, i; Table 1).

The anatomical cluster comprising the 2nd valvifer, the 2nd valvula and the two muscles connecting them (Fig. 5l) is a simple mechanical system in which the 2nd valvula is a two-armed class 1 lever. The ratio of the anatomical inlevers ($a = 66 \mu\text{m}$ and $b = 84 \mu\text{m}$; Fig. 5m) is 1:1.27. The torques (M) of the muscle forces of the anterior and posterior 2nd valvifer-2nd valvula muscle (F_2 and F_3) on the basal articulation in the resting position can be estimated by using the maximum force of the muscle (F ; cf. eq. 1), the lengths of the anatomical inlever arms and the attachment angles of the muscles at the 2nd valvula ($\alpha = 154^\circ$ and $\beta = 96^\circ$; Fig. 5m) according to the equations:

$$M_2 = F_2 \cdot a \cdot \sin(\alpha) \quad (\text{eq. 2})$$

$$M_3 = F_3 \cdot b \cdot \sin(\beta) \quad (\text{eq. 3})$$

However, the lengths of the effective (= mechanical) inlever arms (a' and b' ; Fig. 5m) vary greatly with attachment angle (joint angle), i.e. during the flexion or extension of the terebra. The attachment angle of m3 in the resting position is almost 90° ; thus, the effective inlever arm is almost optimal, so that the force of m3 can be optimally transmitted to the 2nd valvula, which leads to a high torque. By contrast, the attachment angle of m2 in the resting position is far below 90° but increases when the wasp flexes its terebra towards the active probing position. This results in an increase in length of the effective inlever arm, an optimal force transmission of m2 at the basal articulation and consequently a high torque. High torques at the basal articulation might be crucial to enable the extensive movements for both the flexion and extension of the terebra, despite the relatively small anatomical inlevers.

Pro- and retraction of the 1st valvulae

Three muscles (m4–m6) connect the 2nd valvifer with the female T9, both these structures being connected with the 1st valvifer by the intervalvifer

articulation or the tergo-valvifer articulation (iva/tva; 1c, f, g, 4f, j, 5i–k), forming a double joint. The insertion regions at the 2nd valvifer of both parts of the dorsal T9-2nd valvifer muscle (m4a/b) lie anterodorsally, whereas the regions of origin at the female T9 are posterodorsally located of both articulations. A contraction of m4a and m4b (F_4 ; Fig. 5d, i) moves the 2nd valvifer posteriorly and the female T9 anteriorly towards each other (small number 3; Fig. 5c, i), whereby the tension of the posterior T9-2nd valvifer muscle (m6) presumably prevents the involved cuticular elements to rotate around the articulations. This movement causes the 1st valvifer to tilt anteriorly (small number 4; Fig. 5c, i) because it is articulated with both the 2nd valvifer and the female T9 via rotational joints (intervalvifer and tergo-valvifer articulation). The 1st valvifer acts as a one-armed class 3 lever that transfers its tilting movement to the dorsal ramus of the 1st valvula, causing the 1st valvula to slide distally relative to the 2nd valvula (small number 5; Fig. 5c). Both m4a and m4b act as protractors of the 1st valvulae (Table 1). They might also assist in extending the terebra (Fig. 5c), as a simultaneous protraction of the 1st valvulae places the terebra under unilateral tension due to friction between the olistheter elements of the 1st and 2nd valvulae. The origin of the antagonistic ventral T9-2nd valvifer muscle (m5) at the female T9 is situated posterodorsally near the intervalvifer articulation and posterior to the tergo-valvifer articulation, whereas its insertion region at the 2nd valvifer is located posteroventrally of both these articulations. Its contraction (F_5 ; Fig. 5f, i) moves the 2nd valvifer anteriorly with respect to the female T9 (small number 6; Fig. 5e, i), thus indirectly causing the 1st valvifer to tilt posteriorly (small number 7; Fig. 5e, i) and the 1st valvulae, as a direct consequence, to slide proximally relative to the 2nd valvula (small number 8; Fig. 5e). Therefore, m5 acts as a retractor of the 1st valvulae (Table 1). It might also assist in flexing the terebra (Fig. 5e), as a simultaneous retraction of both of the 1st valvulae places the terebra under a unilateral tension due to friction between the olistheter elements of the 1st and 2nd valvulae. Muscles m4a and m4b act antagonistically against m5, i.e. m4a/b protract the 1st valvulae, whereas m5 retracts them. The posterior T9-2nd valvifer muscle (m6) stabilizes the ovipositor system by holding the 2nd valvifer and the female T9 in position and prevents them to rotate around the articulations (Fig. 5d; Table 1), although some limited movements in dorso–ventral direction at their posterior ends are likely to occur (cf. Fig. 4g).

The following assumptions were made for a simplified estimation of the torques (M) of the muscle

forces of the dorsal and ventral T9-2nd valvifer muscle (F_4 and F_5): (1) The 2nd valvifer acts as the frame of reference; therefore, the intervalvifer articulation (iva; Figs. 1c, f, g, 4f, j, 5i, j, k) acts as the pivot point (= joint axis or fulcrum) at which the 1st valvifer tilts; and (2) the 2nd valvifer and the female T9 are guided and cannot twist around the articulations but only move towards to or apart from each other along the horizontal anterior–posterior axis without friction occurring. Under these assumptions, the horizontal force vector components of m_4 and m_5 ($F_{4x} = \cos(\gamma) \cdot F_4$ and $F_{5x} = \cos(\delta) \cdot F_5$ with $\gamma = 5^\circ$ and $\delta = 24^\circ$; Fig. 5j, k) act at the 1st valvifer at the tergo-valvifer articulation (tva; Figs. 1c, f, 4f, j, 5i, j, k). Therefore, the torque (M) of F_{4x} and F_{5x} on the intervalvifer articulation in the resting position can be estimated by using the horizontal vector component (F_x) of the maximum force of a muscle (cf. eq. 1), the length of the anatomical inlever arm ($c = 103 \mu\text{m}$; Fig. 5k)—which is the distance between tergo-valvifer and intervalvifer articulation—and the joint angle ($\varepsilon = 113^\circ$; Fig. 5k) according to the equations:

$$M_4 = F_{4x} \cdot c \cdot \sin(\varepsilon) \quad (\text{eq. 4})$$

$$M_5 = F_{5x} \cdot c \cdot \sin(\varepsilon) \quad (\text{eq. 5})$$

The 1st valvifer acts as a lever with the effective outlever (d' ; Fig. 5k), which is defined as the length between the intervalvifer articulation and the point where the 1st valvifer continues as dorsal ramus of the 1st valvula. The resulting pro- or retracting forces at the dorsal ramus of the 1st valvula (F_{vvm4} and F_{vvm5} ; Fig. 5k) can be estimated by using the horizontal vector components (F_x) of the forces acting on the 1st valvifer at the tergo-valvifer articulation, the length of the effective inlever arm ($c' = c \cdot \sin(\varepsilon) = 94.8 \mu\text{m}$; Fig. 5k) and the effective outlever arm according to the equations:

$$F_{1vv4} = (F_{4x} \cdot c') / d' \quad (\text{eq. 6})$$

$$F_{1vv5} = (F_{5x} \cdot c') / d' \quad (\text{eq. 7})$$

The distance that the 1st valvifer moves is equally transferred to the 1st valvula. Thereby, the shape of the 1st valvifer and the positions of the tergo-valvifer and the intervalvifer articulations influence the way how the 1st valvula is moved, i.e. the more closely the two articulations are situated to each other and the further they are away from the anterior angle of the 1st valvifer, the further the 1st valvula will slide relative to the 2nd valvula along the olistheter [19]. An increase of the quotient of the effective outlever to the effective inlever ($d': c'$ ratio) results in a smaller force output but an increase in the potential maximum velocity and mechanical deflection, i.e. an increase in the speed and the movement distance of the dorsal rami of the 1st valvulae. Their tight interlocking with the dorsal projection of the 2nd valvifer

prevents them from buckling and transfers the movements to the apex of the valvulae. The double joint system of the 1st valvifer enables an pro- and retraction of the 1st valvulae.

The 1st valvifer-genital membrane muscle (m_1) potentially serves as a tensor muscle that stabilizes the 1st valvifers during their fast alternate movements by holding them in position laterally to the 2nd valvifers (Fig. 5a, b; Table 1).

Process of oviposition

After a female wasp has found a suitable oviposition site, the contraction of the posterior 2nd valvifer-2nd valvula muscles (m_3) causes the 2nd valvula and the interlocked 1st valvulae to flex anteriorly towards the active probing position [19]. This flexing and the general employment of the terebra of *V. canescens* (as in many other ichneumonoid wasp taxa [62, 63]) might be assisted by the annulated and flexible 3rd valvulae and the generally improved manoeuvrability of the metasoma of the Apocrita [64]. The 2nd valvifer is then rotated away from the dorsal surface of the metasoma concomitantly with the terebra. During the so-called cocking behaviour (*sensu* [32]) of *V. canescens*, the 2nd valvifer and the terebra flex simultaneously. In *V. canescens*, this characteristic behaviour is always performed prior to the actual oviposition and is assumed to correlate with the egg being passed down into the spindle-shaped cavity at the apex of the terebra in readiness for oviposition [32, 45]. The parasitoid then performs localized probing movements with the unsheathed terebra in the substrate (Additional file 1). Drilling movements of the terebra are not needed, since the hosts of *V. canescens* live in soft substrates. Once a suitable host is found, stabbing movements are conducted, whereby the terebra is quickly inserted into the host caterpillar [32, 65]. Thereby, alternate contractions of the dorsal T9-2nd valvifer muscles (m_4 a/b) and the ventral T9-2nd valvifer muscles (m_5) indirectly execute the penetration movements of the 1st valvulae (which are documented in a braconid wasp [66]). In some species of Braconidae (the sister group of Ichneumonidae), these movements of the 1st valvulae are known to enable the wasps to actively steer their terebra to some extent: asymmetrical apex forces at the terebra in a viscid medium—caused by varying its asymmetrical tip by pro- or retracting one 1st valvula with respect to the other—result in a passive bending of the terebra [66], or restrictions in inter-element displacements (e.g. strongly swollen short regions pre-apically on the rhachises) cause the terebra to bend due to tensile and compressive forces [67]. Throughout penetration,

the relative position of the valvifers and consequently of the 1st valvulae might be monitored via the sensillar patches of the 2nd valvifers situated anteriorly to the intervalvifer articulations. In addition to penetrating the substrate, the longitudinal alternate movements of the 1st valvulae presumably serve to pass the egg along the terebra. This is facilitated by the egg canal microsculpture consisting of distally oriented scales (ctenidia and subctenidial setae) that push the egg towards the apex of the terebra and hold it in position by preventing backward movements [43, 46, 47]. Shah [45] suggests that the valvilli assist in moving the egg in the terminal part of the terebra by using hydrostatic pressure for a speedy delivery of the egg into the host. In *V. canescens*, the laying of an egg into the haemocoel of the host caterpillar takes only a fraction of a second [32, 45]. After oviposition and withdrawal of the terebra, the anterior 2nd valvifer-2nd valvula muscles (m2) extend the terebra back towards its resting position between the internal concave faces of the 3rd valvulae [10]. Oviposition is commonly followed by cleaning behaviour during which the wasp especially grooms its antennae and terebra.

Conclusions

The examination of the elements of the musculoskeletal ovipositor system of *V. canescens* and its underlying working mechanisms adds to our understanding of a key feature in the evolution of parasitoid hymenopterans, a feature that has impacted the evolutionary success of ichneumonid wasps (with more than 24,000 described [68] and more than 100,000 estimated species [69]) and parasitoid hymenopterans in general (with 115,000 described and 680,000 estimated species [70]). Whereas the basic organization of the ovipositor is remarkably uniform among the Hymenoptera [8], huge variations exist in its structure [9, 11, 12], which are associated with the employment of the terebra in the different taxa of parasitoid species (cf. [62, 63, 71, 72]). Further studies that combine thorough morphological analyses of a parasitoid's musculoskeletal ovipositor system with investigations of its parasitoid-host interactions are needed in order to understand how morpho-physiological traits have influenced the evolution of behavioural, ecological and life history traits and *vice versa* in the megadiverse parasitoid Hymenoptera.

Methods

The *V. canescens* specimens used in this study originated from the thelytokous lab colony of Biologische Beratung Ltd. (Berlin, Germany) from whom we also

received larvae of the host *Ephestia kuehniella* Zeller, 1879 (Lepidoptera: Pyralidae). The wasps were kept in a glass box (20 · 30 · 20 cm) and reproduced after the addition of several pyralid larvae within a mealy substrate to the box every third week (Additional file 1). Three times a week, the imagos were fed with watered honey absorbed onto paper towels. The room was kept at a constant temperature of 24°C.

Light microscopy (LM) and scanning electron microscopy (SEM)

The ovipositor was excised and dissected from the genital chamber of ethanol-fixed animals by using fine forceps, macerated in 10% aqueous potassium hydroxide (KOH) for 12–15 h at room temperature if necessary, cleaned in distilled water and dehydrated stepwise in ethanol (C₂H₆O).

For light microscopy, specimens were mounted onto microscopic slides (76 mm · 26 mm, VWR International, Radnor, PA, USA), embedded in Euparal (Waldeck GmbH & Co. KG, Münster, Germany) and, after drying, investigated with a light microscope of the type Zeiss Axioplan (Carl Zeiss Microscopy GmbH, Jena, Germany) equipped with a Nikon D7100 single-lens reflex digital camera (Nikon Corporation, Tokyo, Japan) and the software Helicon Remote version 3.6.2.w (Helicon Soft Ltd., Kharkiv, Ukraine) (for focus stacking Helicon Focus version 6.3.7 Pro; RRID:SCR_014462).

For scanning electron microscopy (SEM), specimens were air-dried for at least one week in a desiccator. The samples were mounted with double-sided adhesive tape onto stubs, sputter-coated with 19 nm pure gold (Au) by using an Emitech K550X (Quorum Technologies Ltd., West Sussex, UK) and investigated with a scanning electron microscope of the type Zeiss EVO LS 10 (Carl Zeiss Microscopy GmbH, Jena, Germany) and the software SmartSEM version V05.04.05.00 (Carl Zeiss Microscopy GmbH, Jena, Germany).

After completion of the microscopical studies, the remaining wasps were killed by freezing them at –20°C.

Synchrotron X-ray phase-contrast microtomography (SR-μCT)

Two metasomas of ethanol-fixed female *V. canescens* were dehydrated stepwise in ethanol and critical-point-dried by using a Polaron 3100 (Quorum Technologies Ltd., West Sussex, UK) to minimize shrinking artefacts by water loss during the tomography procedure. The anterior ends of the metasomas were glued onto the tips of plastic pins, so that the ovipositor tip was oriented upright, and mounted onto the goniometer head of the sample stage for

tomography. Synchrotron X-ray phase-contrast microtomography (SR- μ CT) [73] was performed at the beamline ID19 at the European Synchrotron Radiation Facility (ESRF) (Grenoble, France) at 19 keV (wavelength $8 \cdot 10^{-11}$ m) and an effective detector pixel size of $0.68 \mu\text{m}$ with a corresponding field of view of $1.43 \cdot 1.43 \text{ mm}$; 6000 projections were recorded over the 180 degree rotation. The detector-to-sample distance was 12 mm. As the structures of interest were larger than the field of view, four separate image stacks were acquired. Therefore, the sample was repositioned in between the imaging procedure, resulting in a certain overlap of two consecutive images. The 3D voxel datasets were reconstructed from the 2D radiographs by using the filtered back-projection algorithm [74, 75] developed for absorption contrast tomography.

Registration and segmentation of SR- μ CT images

To obtain a high-resolution 3D image of the ovipositor and the inherent muscles, two consecutive images from the stack were geometrically aligned in an iterative 3D rigid registration procedure (Additional file 3). A stepwise strategy was applied for the registration. The two data sets were aligned according to the translation of the sample stage in between imaging. The images were then rigidly registered by using normalized mutual information of the grey value images as a similarity measure, with a line search algorithm for the optimization approach. A hierarchical strategy was applied to reduce the risk of finding local minima, starting at a coarse resampling of the datasets and proceeding to finer resolutions. Finally, an affine transformation by using a Lanczos interpolation (cf. [76]) was performed that interpolated both images into the same coordinate system. As a result, all four images were matched in a common coordinate system. An edge-preserving smoothing filter was applied for the segmentation of the individual structures. Segmentation was based on local differences in densities, as chitinous structures have higher densities than muscles. Therefore, grey value images were binarized by using a dual threshold approach that allowed the extraction and separation of regions with different densities.

Image processing and extraction of individual morphological structures

The obtained two masks of muscles and denser structures were further processed to differentiate them into their various morphological components. Therefore, a semi-automatic extraction of biological structural features was applied by using geometric

information. First, small islands were removed with an opening filter and, subsequently, the connected components were automatically labelled. Second, the resulting chitinous structures were manually split at the connection points between the female T9 and the valvifers and at the olistheter mechanism of the terebra, as these fine structures could not be segmented automatically because of the limited resolution of the images. For each muscle bundle, insertion regions (apodemes) were identified on the cuticular elements at both muscle ends, with the whole muscle between the apodemes being determined in a semi-automated interpolation process. This resulted in individual labels for the six muscles involved in ovipositor actuation mechanics. A Gaussian filter was applied for smoothing the 3D masks of the individual chitinous and muscular structures and 3D morphological volumetric models of the biological structures were generated.

Image processing was performed by using the software Amira version 6.0 (FEL, Hillsboro, OR, USA; RRID:SCR_014305) and the custom MATLAB scripts version R2016a (The MathWorks, Inc., Natick, MA, USA; RRID:SCR_001622).

Muscle and leverage analyses

Muscle volume, mean length and mean cross section area were determined from the 3D data sets. The obtained muscle volume values potentially are lower than in living animals due to shrinking artefacts. The total muscle length and the major direction of the muscle force was determined as the distance between the centre points of the attachments of the muscles and the direction of the line in between, respectively. The exact locations of the muscles' origins and insertions were verified with light microscopy. The mean cross section area (CSA) was determined as the muscle volume / muscle length. However, the orientation of the single muscle fibre might deviate from the direction of the main muscle force (cf. [77]), which potentially results in an underestimation of the estimated CSA of an individual muscle and thus its maximum muscle force but also an overestimation of its maximum contraction distance. The anatomical inlevers were measured from the 3D data set and the joint angles were determined. The anatomical lever was defined as the length of the line between the joint axis and the point where the muscle force is applied, i.e. the tendon attachment point. The effective lever arm, which is pivotal for the efficiency of the force transmission, is defined as the perpendicular distance between the projection of the line of action of the tendon attachment point and the joint axis.

Appendix

Table 2 Morphological terms relevant to the hymenopteran ovipositor system. The terms (abbreviations used in this article in brackets) are used and defined according to the Hymenoptera Anatomy Ontology (HAO) [5–7]; the respective Uniform Resource Identifiers (URI) and the synonyms found in the cited literature are listed

anatomical term (abbreviation)	definition/concept	URI	synonyms commonly found in literature
1st valvifer (1vf)	The area of the 1st valvifer-1st valvula complex that is proximal to the aulax, bears the 9th tergal condyle of the 1st valvifer and the 2nd valviferal condyle of the 1st valvifer and is connected to the genital membrane by muscle.	http://purl.obolibrary.org/obo/HAO_0000338	1. Valvifer [9]; fulcral plate [20–27]; gonangulum, gonangula [1]; gonocoxite 8 [18]; gonocoxite XIII [13, 14]; kidney plate [60]; triangular plate [8]; vorderer Valvifer [9]; Winkelplatte [17]
1st valvifer-1st valvula complex	The anatomical cluster that is composed of the sclerites that articulates with the 9th abdominal tergite and the 2nd valvifer.	http://purl.obolibrary.org/obo/HAO_0002158	
1st valvifer-2nd valvifer muscle	The ovipositor muscle that arises from the interarticular ridge of the 1st valvifer and inserts on the 2nd valvifer	http://purl.obolibrary.org/obo/HAO_0002189	
1st valvifer-genital membrane muscle (m1)	The ovipositor muscle that arises from the posterior part of the 1st valvifer and inserts anteriorly on the genital membrane anterior to the T9-genital membrane muscle.	http://purl.obolibrary.org/obo/HAO_0001746	anterior tergo-sternal strictor muscle [14]
1st valvula (1vw)	The area of the 1st valvifer-1st valvula complex that is delimited distally by the proximal margin of the aulax.	http://purl.obolibrary.org/obo/HAO_0000339	1. Valvula [9]; gonapophysis 8 [18]; gonapophysis VIII [13, 14]; lancet [8, 60]; lower valve [1, 2, 11, 42, 44, 46, 71, 72]; Stechboiste [9, 17]; stylet [20–27]; ventral stylet [45, 49]; ventral valve [43, 47, 66, 67]; ventral valvula [45, 49]
2nd valvifer (2vf)	The area of the 2nd valvifer-2nd valvula-3rd valvula complex that is proximal to the basal articulation and to the processus musculares and articulates with the female T9.	http://purl.obolibrary.org/obo/HAO_0000927	2. Valvifer [9]; gonocoxite 9 [1, 18]; gonocoxite IX [13, 14]; hinterer Valvifer [9]; inner plate [20]; ~ inner ovipositor plate [21, 22, 24, 26, 27]; oblong plate [8]; oblonge Platte [9, 17]; runner plate [60]; ~ semicircular sheet [23, 25]
2nd valvifer-2nd valvula-3rd valvula complex	The area that is connected to the 9th tergite and the 1st valvifer via conjunctiva, is articulated to the 1st tergite, and bears the aulax.	http://purl.obolibrary.org/obo/HAO_0002175	
2nd valvifer-3rd valvula complex	The area of the 2nd valvifer-2nd valvula-3rd valvula complex that is proximal to the basal articulation.	http://purl.obolibrary.org/obo/HAO_0002181	
2nd valvifer-genital membrane muscle	The ovipositor muscle that arises anteriorly from the dorsal flange of the 2nd valvifer and inserts anteriorly on the dorsal part of the genital membrane.	http://purl.obolibrary.org/obo/HAO_0001672	
2nd valviferal condyle of the 1st valvifer	The condyle that is located on the 1st valvifer and articulates with the 1st valviferal fossa of the 2nd valvifer.	http://purl.obolibrary.org/obo/HAO_0002167	
2nd valvula (2vw)	The area of the 2nd valvifer-2nd valvula-3rd valvula complex that is distal to the basal articulation and to the processus musculares and is limited medially by the median body axis.	http://purl.obolibrary.org/obo/HAO_0000928	2. Valvula [9]; dorsal valve [43, 47, 66, 67]; dorsal stylet [45, 49]; dorsal valvula [45, 49]; gonapophysis 9 [18]; gonapophysis IX [13, 14]; Schienenrinne [9, 17]; sheath [21, 22, 27]; ~ stylet [= slender distal part of the united 2nd valvulae] [8] stylet sheath [20, 23–26]; upper valve [1, 2, 11, 42, 44, 46, 71, 72]; (fused) ventral valves [60]

Table 2 Morphological terms relevant to the hymenopteran ovipositor system. The terms (abbreviations used in this article in brackets) are used and defined according to the Hymenoptera Anatomy Ontology (HAO) [5–7]; the respective Uniform Resource Identifiers (URI) and the synonyms found in the cited literature are listed (Continued)

anatomical term (abbreviation)	definition/concept	URI	synonyms commonly found in literature
3rd valvula (3rv)	The area of the 2nd valvifer-3rd valvula complex that is posterior to the distal vertical conjunctiva of the 2nd valvifer-3rd valvula complex.	http://purl.obolibrary.org/obo/HAO_0001012	3. Valvula [9]; articulating palps [25]; dorsal valve [60]; gonostylus [18]; gonostylus IX [13, 14]; ~ inner ovipositor plate [23]; ovipositor sheath [1, 2, 11, 43–45, 49]; palp [20]; sheath [67]; sheath lobe [8]; Stachelscheide [9, 17]; terminal palp [24]
9th tergal condyle of the 1st valvifer	The condyle that is located on the 1st valvifer and articulates with the 1st valviferal fossa of T9.	http://purl.obolibrary.org/obo/HAO_0002160	
annulus	The carina that is transverse and extends across the lateral wall of the terebra.	http://purl.obolibrary.org/obo/HAO_0001173	
anterior 2nd valvifer-2nd valvula muscle (m2)	The ovipositor muscle that arises from the anterodorsal part of the 2nd valvifer and inserts subapically on the processus articularis.	http://purl.obolibrary.org/obo/HAO_0001166	anterior gonocoxapophysal muscle [13, 14]; gonapophysis 9 levator [18]; ramus muscle of the 2nd valvula [8]; shaft elevator muscle [27]
anterior angle of the 1st valvifer	The corner on the 1st valvifer that marks the posterior end of the 1st valvula.	http://purl.obolibrary.org/obo/HAO_0002168	
anterior area of the 2nd valvifer	The area of the 2nd valvifer which is anterior to the anatomical line that is the shortest distance from the 1st valviferal fossa of the 2nd valvifer and the ventral margin of the 2nd valvifer.	http://purl.obolibrary.org/obo/HAO_0002169	
anterior flange of the 1st valvifer	The flange that extends anteriorly on the 1st valvifer and overlaps with the posterior margin of the anterior area of the 2nd valvifer.	http://purl.obolibrary.org/obo/HAO_0002166	
anterior flange of abdominal tergum 9 (af9)	The flange that extends along the anterolateral margin of female T9.	http://purl.obolibrary.org/obo/HAO_0001171	Apodem [9]
anterior ridge of T9	The ridge that extends along the anterior margin of female T9 and receives the site of origin of the ventral and the dorsal T9-2nd valvifer muscles.	http://purl.obolibrary.org/obo/HAO_0002182	
anterior section of dorsal flange of 2nd valvifer (asdf)	The area of the dorsal flange of the 2nd valvifer that is anterior to the site of origin of the basal line.	http://purl.obolibrary.org/obo/HAO_0002173	~ semicircular sheet [23–27]
apodeme	The process that is internal.	http://purl.obolibrary.org/obo/HAO_0000142	
articular surface	The area that is located on the sclerite and that makes movable direct contact with another sclerite.	http://purl.obolibrary.org/obo/HAO_0001485	
aulax (au)	The impression that is on the 1st valvifer-1st valvula complex accommodates the rhachis.	http://purl.obolibrary.org/obo/HAO_0000152	Falze der Stechborste [17]; groove [20, 21, 25]
basal articulation (ba)	The articulation that is part of the 2nd valvifer-2nd valvula-3rd valvula complex and adjacent to the rhachis.	http://purl.obolibrary.org/obo/HAO_0001177	Basalgelenk [9]; bulbous articulation [18, 21, 25–27]
basal line of the 2nd valvifer	The line on the 2nd valvifer that extends between the pars articularis and the dorsal flange of 2nd valvifer.	http://purl.obolibrary.org/obo/HAO_0002171	

Table 2 Morphological terms relevant to the hymenopteran ovipositor system. The terms (abbreviations used in this article in brackets) are used and defined according to the Hymenoptera Anatomy Ontology (HAO) [5–7]; the respective Uniform Resource Identifiers (URI) and the synonyms found in the cited literature are listed (*Continued*)

anatomical term (abbreviation)	definition/concept	URI	synonyms commonly found in literature
bulb (bib)	The anterior area of the dorsal valve [composite structure of the fused 2nd valvulae] that is bulbous.	http://purl.obolibrary.org/obo/HAO_0002177	Backen [17]; bulbous basal part of the united 2nd valvulae [8]; boubulous sockets [25, 26]; pivoting process [20]; sockets [27]
carina	The process that is elongate and external.	http://purl.obolibrary.org/obo/HAO_0000188	
condyle	The articular surface that is convex and is inserted into the fossa of an adjacent sclerite.	http://purl.obolibrary.org/obo/HAO_0000220	
conjunctiva	The area of the cuticle that is weakly sclerotized, with thin exocuticle.	http://purl.obolibrary.org/obo/HAO_0000221	
cordate apodeme (ca)	The apodeme on the anterior margin of female T9. The ventral T9-2nd valvifer muscle attaches partly on the apodeme.	http://purl.obolibrary.org/obo/HAO_0001585	Apophyse [9]
distal notch of the dorsal valve (no)	The notch that is distal on the dorsal valve [composite structure of the fused 2nd valvulae].	http://purl.obolibrary.org/obo/HAO_0002179	
distal vertical conjunctiva of the 2nd valvifer-3rd valvula complex	The conjunctiva that traverses the 2nd valvifer-3rd valvula complex and is located distal to the median bridge of the 2nd valvifers.	http://purl.obolibrary.org/obo/HAO_0002180	
dorsal flange of the 2nd valvifer	The flange that extends on the dorsal margin of the 2nd valvifer. Part of the ventral T9-2nd valvifer muscle attaches to the flange.	http://purl.obolibrary.org/obo/HAO_0001577	dorsale Verdickungsleiste [9]
dorsal projection of the 2nd valvifer (dp2)	The projection that is located on the 2nd valvifer and corresponds to the proximal end of the rhachis.	http://purl.obolibrary.org/obo/HAO_0002172	~ ramus edge [23, 25, 27]
dorsal ramus of the 1st valvula (dr1)	The region that extends along the dorsal margin of the 1st valvula and bears the aulax.	http://purl.obolibrary.org/obo/HAO_0001579	1st ramus [16]; Ramus der 1. Valvula [9]; ramus of the 1st valvula [8, 51]; Stechborstenbogen [9]
dorsal ramus of the 2nd valvula	The area that extends along the dorsal margin of the 2nd valvula, bears the processus articularis anteriorly and the processus musculares on the antero-dorsal region and articulates with the 2nd valvifer via the basal articulation.	http://purl.obolibrary.org/obo/HAO_0002190	2nd ramus [16]; Ramus der 2. Valvula [9]; Schienenbögen [9, 17]
dorsal sclerite of the 1st valvifer	The sclerite of the 1st valvifer that is located dorsally of the transvalviferal conjunctiva.	http://purl.obolibrary.org/obo/HAO_0002163	
dorsal T9-2nd valvifer muscle (m4a/b)	The ovipositor muscle that arises along the posterodorsal part of the anterior margin of female T9 and inserts on the anterior section of the dorsal flanges of the 2nd valvifer.	http://purl.obolibrary.org/obo/HAO_0001569	anterior tergonocoxal muscle [13, 14]; dorsal/ventral [= part a/part b] anterior tergal muscle of the 2nd valvifer [8]; extensor muscles of lancet [60]; upper/lower [= part a/part b] protractor of gonapophysis 8 [18]; upper/lower [= part a/part b] stylet protractor muscle [27]
dorsal valve	The area that is articulated with the right and left 2nd valvifers at the basal articulation and bears the rhachises. [Term sometimes used for the composite structure of the fused 2nd valvulae.]	http://purl.obolibrary.org/obo/HAO_0001658	[cf. 2nd valvula]

Table 2 Morphological terms relevant to the hymenopteran ovipositor system. The terms (abbreviations used in this article in brackets) are used and defined according to the Hymenoptera Anatomy Ontology (HAO) [5–7]; the respective Uniform Resource Identifiers (URI) and the synonyms found in the cited literature are listed (Continued)

anatomical term (abbreviation)	definition/concept	URI	synonyms commonly found in literature
egg canal (ec)	The anatomical space that is between the left and right olistheter.	http://purl.obolibrary.org/obo/HAO_0002191	Eikanal [9]; Innenkanal [9, 17]
female T9 (T9)	The tergite that is articulated with the 1st valvifer and is connected to the 2nd valvifer via muscles.	http://purl.obolibrary.org/obo/HAO_0000075	9. Tergit [9]; 9th tergum [8]; outer ovipositor plate [21–27]; outer plate [20]; quadrat plate [8]; quadratische Platte [9, 17]; sled plate [60]; T9 [1, 10, 15, 19, 51, 52]; terga 9 [45, 49]; tergite 9 [12, 18]; tergite IX [13, 14]; tergum 9 [10, 15, 51, 52]; tergum IX [16]
flange	The projection that is lamella-like and is located on a rim, carina, apodeme or edge.	http://purl.obolibrary.org/obo/HAO_0000344	
fossa	The articular surface that is concave and accommodates the condyle of another sclerite.	http://purl.obolibrary.org/obo/HAO_0000353	
furcula	The sclerite that is proximal to the 2nd valvifer and receives the site of origin of the posterior 2nd valvifer-2nd valvula muscle.	http://purl.obolibrary.org/obo/HAO_0002498	Gabelbein [9]
genital membrane	The conjunctiva that connects the ventral margins of the 2nd valvifers arching above the 2nd valvula.	http://purl.obolibrary.org/obo/HAO_0001757	
integument	The anatomical system that forms the covering layer of the animal, ectodermal in origin and composed of epidermal cells producing the cuticle.	http://purl.obolibrary.org/obo/HAO_0000421	
interarticular ridge of the 1st valvifer (iar)	The ridge that extends along the posterior margin of the 1st valvifer between the intervalvifer and tergovavifer articulations.	http://purl.obolibrary.org/obo/HAO_0001562	
intervalvifer articulation (iva)	The articulation between the 1st valvifer and 2nd valvifer.	http://purl.obolibrary.org/obo/HAO_0001558	Intervalviferengelenk [9]
intravalvifer articulation	The articulation between the dorsal sclerite of the 1st valvifer and the ventral sclerite of the 1st valvifer.	http://purl.obolibrary.org/obo/HAO_0002165	
lateral T9-2nd valvifer muscle	The muscle arises from the posteroventral parts of the female T9 and inserts on the median bridge.	http://purl.obolibrary.org/obo/HAO_0002187	
median bridge of the 2nd valvifers (mb2)	The area that connects posterodorsally the 2nd valvifers and is the site of attachment for the posterior T9-2nd valvifer muscle.	http://purl.obolibrary.org/obo/HAO_0001780	
medial conjunctiva of the 1st valvula	The conjunctiva that extends medially along the 1st valvula.	http://purl.obolibrary.org/obo/HAO_0002192	
medial conjunctiva of abdominal tergum 9	The conjunctiva of abdominal tergum 9 that has median and longitudinal.	http://purl.obolibrary.org/obo/HAO_0002267	
notal membrane (nm)	The conjunctiva that connects the medial margins of the 2nd valvulae.	http://purl.obolibrary.org/obo/HAO_0001733	
olistheter (oth)	The anatomical cluster that is composed of the rhachis of the 2nd valvula and the aulax of the 1st valvula.	http://purl.obolibrary.org/obo/HAO_0001103	

Table 2 Morphological terms relevant to the hymenopteran ovipositor system. The terms (abbreviations used in this article in brackets) are used and defined according to the Hymenoptera Anatomy Ontology (HAO) [5–7]; the respective Uniform Resource Identifiers (URI) and the synonyms found in the cited literature are listed (*Continued*)

anatomical term (abbreviation)	definition/concept	URI	synonyms commonly found in literature
ovipositor	The anatomical cluster that is composed of the 1st valvulae, 2nd valvulae, 3rd valvulae, 1st valvifers, 2nd valvifers and female T9.	http://purl.obolibrary.org/obo/HAO_0000679	ovipositor mechanism [27]
ovipositor apparatus	The anatomical cluster that is composed of the ovipositor, abdominal terga 8–10, abdominal sternum 7 and muscles connecting them.	http://purl.obolibrary.org/obo/HAO_0001600	
ovipositor muscle	The abdominal muscle that inserts on the ovipositor.	http://purl.obolibrary.org/obo/HAO_0001290	
pars articularis	The articular surface that is situated anteriorly on the ventral margin of the 2nd valvifer and forms the lateral part of the basal articulation.	http://purl.obolibrary.org/obo/HAO_0001606	
posterior 2nd valvifer-2nd valvula muscle (m3)	The ovipositor muscle that arises posteroventrally from the 2nd valvifer and inserts on the processus musculares of the 2nd valvula.	http://purl.obolibrary.org/obo/HAO_0001815	gonapophysis 9 depressor [18]; muscle of the furcula [in the Ichneumonid <i>Megarhyssa</i>] [8]; posterior gonocoxapophyseal muscle [13, 14]; retractor of ventral valves [60]
posterior area of the 2nd valvifer	The area of the 2nd valvifer that is posterior to the anatomical line that is the shortest distance from the valviferal fossa of the 2nd valvifer to the ventral margin of the 2nd valvifer.	http://purl.obolibrary.org/obo/HAO_0002170	
posterior margin of 1st valvifer	The margin of the 1st valvifer that is posterior and extends between the intervalvifer articulation and the anterior angle of the 1st valvifer.	http://purl.obolibrary.org/obo/HAO_0002159	~ inner ovipositor plate [23–27]
posterior section of dorsal flange of 2nd valvifer (psdf)	The area of the dorsal flange of the 2nd valvifer that is posterior to the site of origin of the basal line.	http://purl.obolibrary.org/obo/HAO_0002174	dorsal/lateral tergo-gonostylar muscle [13, 14]; posterior dorso-ventral muscle [60]
posterior T9-2nd valvifer muscle (m6)	The ovipositor muscle that arises medially from the posterodorsal part of female T9 and inserts on the median bridge of the 2nd valvifers.	http://purl.obolibrary.org/obo/HAO_0001813	
posteroventral corner of the 1st valvifer	The corner of the 1st valvifer that is adjacent to the intervalvifer articulation.	http://purl.obolibrary.org/obo/HAO_0002239	
process	The area on the sclerite that is raised.	http://purl.obolibrary.org/obo/HAO_0000822	
processus articularis (pra)	The process that extends laterally from the proximal part of the 2nd valvula and forms the median part of the basal articulation, and corresponds to the site of attachment for the anterior 2nd valvifer-2nd valvula muscle.	http://purl.obolibrary.org/obo/HAO_0001704	
processus musculares (prm)	The apodeme that extends dorsally from the proximal part of the 2nd valvula to the genital membrane and receives the site of attachment of the posterior 2nd valvifer-2nd valvula muscle.	http://purl.obolibrary.org/obo/HAO_0001703	
rhachis (rh)	The ridge that extends along the ventral surface of the 2nd valvula that is partially enclosed by the aulax.	http://purl.obolibrary.org/obo/HAO_0000898	Leisten der Schienenrinne [17]; T-ridge of ventral valve [60]
ridge	The apodeme that is elongate.	http://purl.obolibrary.org/obo/HAO_0000899	

Table 2 Morphological terms relevant to the hymenopteran ovipositor system. The terms (abbreviations used in this article in brackets) are used and defined according to the Hymenoptera Anatomy Ontology (HAO) [5–7]; the respective Uniform Resource Identifiers (URI) and the synonyms found in the cited literature are listed (*Continued*)

anatomical term (abbreviation)	definition/concept	URI	synonyms commonly found in literature
sawtooth (st)	The process that is located along the ventral margin of the 1st valvula or the dorsal margin of the 2nd valvula.	http://purl.obolibrary.org/obo/HAO_0001681	barb, barbs [43]; teeth [23–26]; Sägezähnen [9, 17]; sheath teeth [21]; Zähnen [9]
sclerite	The area of the cuticle that is strongly sclerotized, with thick exocuticle and is surrounded by conjunctivae.	http://purl.obolibrary.org/obo/HAO_0000909	
sensillar patch of the 2nd valvifer (sp)	The patch that is composed of placoid sensilla adjacent to the intervalvifer articulation.	http://purl.obolibrary.org/obo/HAO_0001671	Sinneshäärchen des Intervalviferengelenkes [9]
sternum	The area that is located on the integument and is ventral of the ventral diaphragm.	http://purl.obolibrary.org/obo/HAO_0000956	
T9-genital membrane muscle	The ovipositor muscle that arises from the cordate apodeme and inserts dorsally on the proximal part of the genital membrane and on the opposite cordate apodeme.	http://purl.obolibrary.org/obo/HAO_0001639	
tendon	The portion of tissue that is fibrous, strong, composed of tendon cells and connects the muscle to the integument.	http://purl.obolibrary.org/obo/HAO_0000996	
terebra (trb)	The anatomical cluster that is composed of the 1st and 2nd valvulae.	http://purl.obolibrary.org/obo/HAO_0001004	Legebohrer [17]; ovipositor [1, 11, 18, 42–44, 49, 66, 67, 71, 72]; (ovipositor) shaft [12, 21–27, 45, 47, 56]; shaft of ovipositor [8]; sting shaft [48]; stylus (of the ovipositor) [63]
tergite	The sclerite that is located on the tergum.	http://purl.obolibrary.org/obo/HAO_0001005	
tergo-valvifer articulation (tva)	The articulation that is located between the female T9 and the 1st valvifer and is composed of the 9th tergal condyle of the 1st valvifer and the 1st valviferal fossa of the 9th tergite.	http://purl.obolibrary.org/obo/HAO_0001636	Tergovalviferengelenk [9]
tergum	The area that is located on the integument and is dorsal of the ventral diaphragm.	http://purl.obolibrary.org/obo/HAO_0001006	
transvalviferal conjunctiva	The conjunctiva that transverses the 1st valvifer and separates the dorsal and ventral sclerites of the 1st valvifer.	http://purl.obolibrary.org/obo/HAO_0002162	
valvillus (vlv)	The sclerite that articulates on the 1st valvula and projects into the egg/poison canal.	http://purl.obolibrary.org/obo/HAO_0001619	Hemmplättchen [9]; projection [32]
venom gland reservoir of the 2nd valvifer	The gland reservoir that is between the 2nd valvifers.	http://purl.obolibrary.org/obo/HAO_0002176	
ventral ramus of the 1st valvula	The area that extends external to the dorsal ramus of the 1st valvula.	http://purl.obolibrary.org/obo/HAO_0000891	Ventralfortsatz [9]
ventral ramus of the 2nd valvula	The area of the 2nd valvifer-2nd valvula-3rd valvula complex that bears the rhachis.	http://purl.obolibrary.org/obo/HAO_0001107	
ventral sclerite of the 1st valvifer	The sclerite of the 1st valvifer that is ventral to the transvalviferal conjunctiva.	http://purl.obolibrary.org/obo/HAO_0002164	

Table 2 Morphological terms relevant to the hymenopteran ovipositor system. The terms (abbreviations used in this article in brackets) are used and defined according to the Hymenoptera Anatomy Ontology (HAO) [5–7]; the respective Uniform Resource Identifiers (URI) and the synonyms found in the cited literature are listed (*Continued*)

anatomical term (abbreviation)	definition/concept	URI	synonyms commonly found in literature
ventral T9-2nd valvifer muscle (m5)	The ovipositor muscle that arises from the lateral region of female T9 and inserts along the posterior part of the dorsal flange of the 2nd valvifer.	http://purl.obolibrary.org/obo/HAO_0001616	gonapophysis 8 retractor [18]; posterior tergal muscle of the 2nd valvifer [8]; posterior tergonocoxal muscle [13, 14]; retractor muscle of lancet [65]; stylet retractor muscle [27]

Additional files

Additional file 1: Video sequence of female *Venturia canescens* probing with their terebra in a mealy substrate and potential egg injection into a host larvae (*Ephestia kuehniella*). (MP4 19585 kb)

Additional file 2: Animation of the rotating segmented 3D model of the ovipositor of *Venturia canescens*. (MP4 12464 kb)

Additional file 3: Registered SR- μ CT images of the section of the metasoma of *Venturia canescens* that contains the musculoskeletal ovipositor system and animation of the surface rendering of the aligned SR- μ CT data. (MP4 11892 kb)

Abbreviations

1vf: 1st valvifer; 1vv: 1st valvula; 2vf: 2nd valvifer; 2vv: 2nd valvula; 3vv: 3rd valvula; af9: Anterior flange of T9; asdf: Anterior section of the dorsal flange of the 2nd valvifer; au: Aulax; ba: Basal articulation; bl: Basal line; blb: Bulb; ca: Cordate apodeme; cs: Campaniform sensilla; ct: Ctenidium; dp2: Dorsal projection of the 2nd valvifer; dr1: Dorsal ramus of the 1st valvula; ec: Egg canal; F: Force; F_x : Horizontal vector components of a force; hsl: Hook-shaped lobe of the 2nd valvifer; iar: Interarticular ridge of the 1st valvifer; iva: Intervalvifer articulation; lf1: Longitudinal flap of the 1st valvula; M: Torque; m1: 1st valvifer-genital membrane muscle; m2: Anterior 2nd valvifer-2nd valvula muscle; m3: Posterior 2nd valvifer-2nd valvula muscle; m4a: Dorsal T9-2nd valvifer muscle part a; m4b: Dorsal T9-2nd valvifer muscle part b; m5: Ventral T9-2nd valvifer muscle; m6: Posterior T9-2nd valvifer muscle; mb2: Median bridge of the 2nd valvifers; nm: Notal membrane; no: Notch; oth: Olistheter; pra: Processus articularis; prn: Processus musculares; psdf: Posterior section of the dorsal flange of the 2nd valvifer; rh: Rhachis; sc: Scales; scts: Subscenidial seta; SEM: Scanning electron microscopy; sp: Sensillar patch of the 2nd valvifer; SR- μ CT: Synchrotron X-ray phase-contrast microtomography; ssc: Spindle-shaped cavity in the distal part of the terebra; st: Sawtooth; T6: 6th abdominal tergum; T7: 7th abdominal tergum; T8: 8th abdominal tergum; T9: Female T9 (9th abdominal tergum); T10: 10th abdominal tergum; tm4b: Tendon of the dorsal T9-2nd valvifer muscle part b; trb: Terebra; tva: Tergo-valvifer articulation; vd: Duct of the venom gland reservoir of the 2nd valvifer; vlv: Valvillus

Acknowledgements

The authors thank the following colleagues for their help: Alexander Rack for assistance with the beamline ID19 at ESRF, Monika Meinert and Michael Csader with SEM, Paavo Bergmann, Manfred Drack and Stefan Fischer for valuable tips and inspiring discussions, Helen A. Eggenberger and Theresa Jones for improvements and linguistic corrections of the manuscript, and two referees for their useful comments.

Funding

This work was funded by the German Research Foundation (DFG) as part of the Transregional Collaborative Research Centre (SFB-TRR) 141 'Biological design and integrative structures' (project A03 'Inspired by plants and animals: actively actuated rod-shaped structures exhibiting adaptive stiffness and joint-free kinematics'). The experiment (LS-2342) at ESRF was funded by the EU. The article processing charge was covered by the DFG and the Open Access Publishing Fund of the University of Tübingen.

Availability of data and materials

All data supporting the conclusions of this article are included within the article and its additional files. The analysed raw datasets are available from the corresponding author on reasonable request.

Authors' contributions

BE, AIB, OR and OB prepared the study design. OB attained the SR- μ CT data. AIB performed the analysis of the SR- μ CT data. BE performed the LM and SEM studies, interpreted the data and wrote the manuscript. AIB, OR and OB discussed the results and revised the manuscript. All authors read and approved the final manuscript.

Ethics approval and consent to participate

No approval of research ethics committees was required to accomplish the goals of this study because experimental work was conducted with an unregulated invertebrate species.

Consent for publication

Not applicable.

Competing interests

The authors declare that they have no competing or financial interests.

Publisher's Note

Springer Nature remains neutral with regard to jurisdictional claims in published maps and institutional affiliations.

Author details

¹Evolutionary Biology of Invertebrates, Institute of Evolution and Ecology, University of Tübingen, Auf der Morgenstelle 28, 72076 Tübingen, Germany.

²Continuum Biomechanics and Mechanobiology, Institute of Applied Mechanics, University of Stuttgart, Pfaffenwaldring 7, 70569 Stuttgart, Germany.

Received: 18 March 2018 Accepted: 16 October 2018

Published online: 12 November 2018

References

1. Quicke DLJ. The braconid and ichneumonid parasitoid wasps: biology, systematics, evolution and ecology. 1st ed. Wiley-Blackwell: Chichester; 2015.
2. Quicke DLJ, LeRalec A, Vilhelmsen L. Ovipositor structure and function in the parasitic Hymenoptera with an exploration of new hypotheses. *Rendiconti*. 1999;47:197–239.
3. Quicke DLJ. Parasitic wasps. 1st ed. London: Chapman & Hall; 1997.
4. Gauld I, Bolton B, editors. The Hymenoptera. 1st ed. Oxford: Oxford University Press; 1988.
5. Yoder MJ, Mikó I, Seltmann KC, Bertone MA, Deans AR. A gross anatomy ontology for Hymenoptera. *PLoS ONE*. 2010;5:e15991.
6. Seltmann KC, Yoder MJ, Mikó I, Forshage M, Bertone MA, Agosti D, et al. A hymenopterists' guide to the Hymenoptera Anatomy Ontology: utility, clarification, and future directions. *J Hymenopt Res*. 2012;27:67–88.
7. Hymenoptera Anatomy Consortium. Hymenoptera Anatomy Ontology. 2018. <http://glossary.hymao.org>. Accessed 28 May 2018.
8. Snodgrass RE. Morphology of the insect abdomen. Part II. The genital ducts and the ovipositor. *Smithson Misc Collect*. 1933;89:1–148.
9. Oeser R. Vergleichend-morphologische Untersuchungen über den Ovipositor der Hymenopteren. *Mitt Zool Mus Berlin*. 1961;37:3–119.
10. Vilhelmsen L. The ovipositor apparatus of basal Hymenoptera (Insecta): phylogenetic implications and functional morphology. *Zool Scr*. 2000;29:319–45.
11. Quicke DLJ, Fitton MG, Tunstead JR, Ingram SN, Gaitens PV. Ovipositor structure and relationships within the Hymenoptera, with special reference to the Ichneumonoidea. *J Nat Hist*. 1994;28:635–82.
12. LeRalec A, Rabasse JM, Wajnberg E. Comparative morphology of the ovipositor of some parasitic Hymenoptera in relation to characteristics of their hosts. *Can Entomol*. 1996;128:413–33.
13. Smith EL. Evolutionary morphology of the external insect genitalia. 2. Hymenoptera. *Ann Entomol Soc Am*. 1970;63:1–27.
14. Smith EL. Biosystematics and morphology of Symphyta—III External genitalia of *Euura* (Hymenoptera: Tenthredinidae): sclerites, sensilla, musculature, development and oviposition behavior. *Int J Insect Morphol Embryol*. 1972;1:321–65.
15. Vilhelmsen L, Isidoro N, Romani R, Basibuyuk HH, Quicke DLJ. Host location and oviposition in a basal group of parasitic wasps: the subgenital organ, ovipositor apparatus and associated structures in the Orussidae (Hymenoptera, Insecta). *Zoomorphology*. 2001;121:63–84.
16. Kumpanenko AS, Gladun DV. Functional morphology of the sting apparatus of the spider wasp *Cryptocheilus versicolor* (Scopoli, 1763) (Hymenoptera: Pompilidae). *Entomol Sci*. 2018;21:124–32.
17. Frühauf E. Legeapparat und Eiablage bei Gallwespen (Cynipidae). *Z Wiss Zool*. 1924;121:656–723.
18. Fergusson NDM. A comparative study of the structures of phylogenetic importance of female genitalia of the Cynipoidea (Hymenoptera). *Syst Entomol*. 1988;13:13–30.
19. Ernst AF, Mikó I, Deans AR. Morphology and function of the ovipositor mechanism in Ceraphronoidea (Hymenoptera, Apocrita). *J Hymenopt Res*. 2013;33:25–61.

20. Hanna AD. The male and female genitalia and the biology of *Euchalcidia anyobori* Hanna (Hymenoptera, Chalcidoidea). *Trans R Entomol Soc Lond.* 1934;82:107–36.
21. King PE. The muscular structure of the ovipositor and its mode of function in *Nasonia vitripennis* (Walker) (Hymenoptera: Pteromalidae). *Proc R Entomol Soc Lond Ser A Gen Entomol.* 1962;37:121–8.
22. King PE, Copland MJW. The structure of the female reproductive system in the Mymaridae (Chalcidoidea: Hymenoptera). *J Nat Hist.* 1969;3:349–65.
23. Copland MJW, King PE. The structure of the female reproductive system in the Eurytomidae (Chalcidoidea: Hymenoptera). *J Zool.* 1972;166:185–212.
24. Copland MJW, King PE. The structure of the female reproductive system in the Torymidae (Hymenoptera: Chalcidoidea). *Trans R Entomol Soc Lond.* 1972;124:191–212.
25. Copland MJW, King PE. The structure of the female reproductive system in the Pteromalidae (Chalcidoidea: Hymenoptera). *Entomol.* 1972;105:77–96.
26. Copland MJW, King PE, Hill DS. The structure of the female reproductive system in the Agaonidae (Chalcidoidea, Hymenoptera). *J Entomol Ser A Gen Entomol.* 1973;48:25–35.
27. Copland MJW. Female reproductive system of the Aphelinidae (Hymenoptera: Chalcidoidea). *Int J Insect Morphol Embryol.* 1976;5:151–66.
28. Roberts HLS, Schmidt O. Lifetime egg maturation by host-deprived *Venturia canescens*. *J Insect Physiol.* 2004;50:195–202.
29. Casas J, Driessen G, Mandon N, Wielard S, Desouhant E, van Alphen J, et al. Energy dynamics in a parasitoid foraging in the wild. *J Anim Ecol.* 2003;72:691–7.
30. Beling I. Zur Biologie von *Nemeritis canescens* Grav. (Hymen. Ophion). I. Züchtungsverfahren und ökologische Beobachtungen. *Z Angew Entomol.* 1932;19:223–49.
31. Salt G. The hosts of *Nemeritis canescens*, a problem in the host specificity of insect parasitoids. *Ecol Entomol.* 1976;1:63–7.
32. Rogers D. The ichneumon wasp *Venturia canescens*: oviposition and avoidance of superparasitism. *Entomol Exp Appl.* 1972;15:190–4.
33. Salt G. Experimental studies in insect parasitism. XIII. The haemocytic reaction of a caterpillar to eggs of its habitual parasite. *Proc R Soc Lond Ser B Biol Sci.* 1965;162:303–18.
34. Salt G. Experimental studies in insect parasitism. XIV. The haemocytic reaction of a caterpillar to larvae of its habitual parasite. *Proc R Soc Lond Ser B Biol Sci.* 1966;165:155–78.
35. Rotheram S. The surface of the egg of a parasitic insect. I. the surface of the egg and first instar larva of *Nemeritis*. *Proc R Soc Lond Ser B Biol Sci.* 1973; 183:179–94.
36. Rotheram S. The surface of the egg of a parasitic insect. II. The ultrastructure of the particulate coat on the egg of *Nemeritis*. *Proc R Soc Lond Ser B Biol Sci.* 1973;183:195–204.
37. Feddersen I, Sander K, Schmidt O. Virus-like particles with host protein-like antigenic determinants protect an insect parasitoid from encapsulation. *Experientia.* 1986;42:1278–81.
38. Beukeboom LW, Driessen G, Luckerhoff L, Bernstein C, Lapchin L, van Alphen JJM. Distribution and relatedness of sexual and asexual *Venturia canescens* (Hymenoptera). *Proc Sect Exp Appl Entomol Neth Entomol Soc.* 1999;10:23–8.
39. Beukeboom LW, Pijnacker LP. Automictic parthenogenesis in the parasitoid *Venturia canescens* (Hymenoptera: Ichneumonidae) revisited. *Genome.* 2000; 43:939–44.
40. Schneider MV, Beukeboom LW, Driessen G, Lapchin L, Bernstein C, van Alphen JJM. Geographic distribution and genetic relatedness of sympatric thelytokous and arrhenotokous populations of the parasitoid *Venturia canescens* (Hymenoptera). *J Evol Biol.* 2002;15:191–200.
41. Amat I, Castelo M, Desouhant E, Bernstein C. The influence of temperature and host availability on the host exploitation strategies of sexual and asexual parasitic wasps of the same species. *Oecologia.* 2006;148:153–61.
42. Belshaw R, Grafen A, Quicke DLJ. Inferring life history from ovipositor morphology in parasitoid wasps using phylogenetic regression and discriminant analysis. *Zool J Linnean Soc.* 2003;213–28.
43. Boring CA, Sharkey MJ, Nychka JA. Structure and functional morphology of the ovipositor of *Homolobus truncator* (Hymenoptera: Ichneumonoidea: Braconidae). *J Hymenopt Res.* 2009;18:1–24.
44. Shaw MR. Further notes on the biology of *Pseudavga flavicoxa* Tobias, 1964 (Hymenoptera, Braconidae, Rhysipolidae). *J Hymenopt Res.* 2017;54:113–28.
45. Shah ZA, Blackwell A, Hubbard SF. Ultramorphology of the ovipositor of *Venturia canescens* (Gravenhorst) and possible mechanisms for oviposition. *Int J Agric Biol.* 2012;14:908–14.
46. Rahman MH, Fitton MG, Quicke DLJ. Ovipositor internal microsculpture in the Braconidae (Insecta, Hymenoptera). *Zool Scr.* 1998;27:319–31.
47. Austin AD, Browning TO. A mechanism for movement of eggs along insect ovipositors. *Int J Insect Morphol Embryol.* 1981;10:93–108.
48. Bender JC. Anatomy and histology of the female reproductive organs of *Habrobracon jugnalis* (Ashmead) (Hymenoptera, Braconidae). *Ann Entomol Soc Am.* 1943;36:537–45.
49. Shah ZA. Morphology, ultrastructure, and probable functions of the sense organs on the ovipositor stylets of the hymenopteran parasitoid, *Venturia canescens* (Gravenhorst). *Microsc Res Tech.* 2012;75:876–83.
50. Vilhelmsen L. Flexible ovipositor sheaths in parasitoid Hymenoptera (Insecta). *Arthropod Struct Dev.* 2003;32:277–87.
51. Matushkina NA. Sting microsculpture in the digger wasp *Bembix rostrata* (Hymenoptera, Crabronidae). *J Hymenopt Res.* 2011;21:41–52.
52. Matushkina NA, Stetsun HA. Morphology of the sting apparatus of the digger wasp *Oxybelus uniglumis* (Linnaeus, 1758) (Hymenoptera, Crabronidae), with emphasis on intraspecific variability and behavioural plasticity. *Insect Syst Evol.* 2016;47:347–62.
53. Andersen SO, Weis-Fogh T. Resilin. A rubberlike protein in arthropod cuticle. *Adv Insect Physiol.* 1964;2:1–65.
54. Qin G, Hu X, Cebe P, Kaplan DL. Mechanism of resilin elasticity. *Nat Commun.* 2012;3:1003.
55. Michels J, Gorb SN. Detailed three-dimensional visualization of resilin in the exoskeleton of arthropods using confocal laser scanning microscopy. *J Microsc.* 2012;245:1–16.
56. Dethier VG. The response of hymenopterous parasites to chemical stimulation of the ovipositor. *J Exp Zool.* 1947;105:199–207.
57. Alexander RM. The maximum forces exerted by animals. *J Exp Biol.* 1985; 115:231–8.
58. Rospars J-P, Meyer-Vernet N. Force per cross-sectional area from molecules to muscles: a general property of biological motors. *R Soc Open Sci.* 2016;3: 160313.
59. Josephson RK, Ellington CP. Power output from a flight muscle of the bumblebee *Bombus terrestris*. I. Some features of the dorso-ventral flight muscle. *J Exp Biol.* 1997;200:1241–6.
60. Abbott CE. How *Megarhyssa* deposits her eggs. *J New York Entomol Soc.* 1934;42:127–33.
61. Peters RS, Krogmann L, Mayer C, Donath A, Gunkel S, Meusemann K, et al. Evolutionary history of the Hymenoptera. *Curr Biol.* 2017;27:1013–8.
62. Heatwole H, Davis DM, Wenner AM. The behaviour of *Megarhyssa*, a genus of parasitic hymenopterans (Ichneumonidae: Ephyialinae). *Z Tierpsychol.* 1962;19:652–64.
63. Le Lannic J, Nénon J-P. Functional morphology of the ovipositor in *Megarhyssa atrata* (Hymenoptera, Ichneumonidae) and its penetration into wood. *Zoomorphology.* 1999;119:73–9.
64. Vilhelmsen L, Mikó I, Krogmann L. Beyond the wasp-waist: structural diversity and phylogenetic significance of the mesosoma in apocritan wasps (Insecta: Hymenoptera). *Zool J Linnean Soc.* 2010;159:22–194.
65. Williams JR. The factors which promote and influence the oviposition of *Nemeritis canescens* Grav. (Ichneumonidae, Ophioninae). *Proc R Entomol Soc Lond Ser A Gen Entomol.* 1951;26:49–58.
66. Cerkvenik U, van de Straat B, Gusseklo SWS, van Leeuwen JL. Mechanisms of ovipositor insertion and steering of a parasitic wasp. *Proc Natl Acad Sci USA.* 2017;114:E7822–31.
67. Quicke DLJ, Fitton MG, Harris J. Ovipositor steering mechanisms in braconid wasps. *J Hymenopt Res.* 1995;4:110–20.
68. Yu DS, van Achterberg K, Horstmann K. World Ichneumonoidea 2004. Taxonomy, biology, morphology and distribution. 2004. <http://www.taxapad.com>. Accessed 22 Jan 2018.
69. Gauld I, Sithole R, Gómez JU, Godoy C. The Ichneumonidae of Costa Rica, 4. *Mem Am Entomol Inst.* 2002;66:1–768.
70. Heraty JM. Parasitoid biodiversity and insect pest management. In: Footitt RG, Adler PH, editors. *Insect biodiversity: science and society*. 1st ed. Oxford: Wiley-Blackwell; 2009. p. 445–62.
71. Fritzen NR, Sääksjärvi IE. Spider silk felting—functional morphology of the ovipositor tip of *Clitopyga* sp. (Ichneumonidae) reveals a novel use of the hymenopteran ovipositor. *Biol Lett.* 2016;12:20160350.
72. Takasuka K, Fritzen NR, Tanaka Y, Matsumoto R, Maeto K, Shaw MR. The changing use of the ovipositor in host shifts by ichneumonid ectoparasitoids of spiders (Hymenoptera, Ichneumonidae, Pimplinae). *Parasite.* 2018;25:17.

73. Betz O, Wegst U, Weide D, Heethoff M, Helfen L, Lee WK, et al. Imaging applications of synchrotron X-ray phase-contrast microtomography in biological morphology and biomaterials science. I. General aspects of the technique and its advantages in the analysis of millimetre-sized arthropod structure. *J Microsc.* 2007;227:51–71.
74. Cloetens P, Pateyron-Salomé M, Buffière JY, Peix G, Baruchel J, Peyrin F, et al. Observation of microstructure and damage in materials by phase sensitive radiography and tomography. *J Appl Phys.* 1997;81:5878–86.
75. Cloetens P, Ludwig W, Boller E, Helfen L, Salvo L, Mache R, et al. Quantitative phase contrast tomography using coherent synchrotron radiation. In: Bonse U, editor. *Proceedings of SPIE: developments in X-ray tomography III*, vol. 4503. Bellingham, WA: SPIE Press; 2002. p. 82–91.
76. Birkhold AI, Razi H, Weinkamer R, Duda GN, Checa S, Willie BM. Monitoring in vivo (re)modeling: a computational approach using 4D microCT data to quantify bone surface movements. *Bone.* 2015;75:210–21.
77. Weihmann T, Kleinteich T, Gorb SN, Wipfler B. Functional morphology of the mandibular apparatus in the cockroach *Periplaneta americana* (Blattodea: Blattellidae) – a model species for omnivore insects. *Arthropod Syst Phylogeny.* 2015;73:477–88.

Ready to submit your research? Choose BMC and benefit from:

- fast, convenient online submission
- thorough peer review by experienced researchers in your field
- rapid publication on acceptance
- support for research data, including large and complex data types
- gold Open Access which fosters wider collaboration and increased citations
- maximum visibility for your research: over 100M website views per year

At BMC, research is always in progress.

Learn more biomedcentral.com/submissions

